Topological Sensitivity Analysis

A. A. Novotny[a], **R. A. Feijóo**[a], **E. Taroco**[a] **& C. Padra**[b]

[a] *Laboratório Nacional de Computação Científica LNCC/MCT,*
Av. Getúlio Vargas 333, 25651-075 Petrópolis - RJ, Brasil
[b] *Centro Atómico Bariloche, 8400 Bariloche, Argentina*

Abstract

The so-called Topological Derivative concept has been seen as a powerful framework to obtain the optimal topology for several engineering problems. This derivative characterizes the sensitivity of the problem when a small hole is created at each point of the domain. However, the greatest limitation of this methodology is that when a hole is created it is impossible to build a homeomorphic map between the domains in study (because they have not the same topology). Therefore, some specific mathematical framework should be developed in order to obtain the derivatives. This work proposes an alternative way to compute the Topological Derivative based on the Shape Sensitivity Analysis concepts. The main feature of this methodology is that all the mathematical procedure already developed in the context of Shape Sensitivity Analysis may be used in the calculus of the Topological Derivative. This idea leads to a more simple and constructive formulation than the ones found in the literature. Further, to point out the straightforward use of the proposed methodology, it is applied for solving some design problems in steady-state heat conduction.

keywords: Topological Derivative, Topological-Shape Sensitivity Analysis, Shape Sensitivity Analysis, Topology Optimization.

1 Introduction

Many physics phenomena can be modelled by a set of partial differential equations with proper boundary conditions (boundary-value problem) or by its equivalent weak form defined over a certain domain. A question of great importance, that has awaken a lot of interest in recent years, is the ability to obtain automatically, in agreement with some measure of performance (cost function), the optimal geometry of the domain of definition of the problem under analysis. Conceptually, the problem is to find the domain, *i.e.* its shape and/or topology such that the cost functional is minimized subject to constraints imposed by, for example, the boundary-value problem. An already established method in the literature that addresses this kind of problems is to parameterize the domain of interest followed by an optimization with respect to these parameters. This leads to the well-known shape optimization technique. The inconvenience of this approach is that the topology is fixed throughout the optimization process. In order to overcome this limitation, topology optimization techniques were developed where very little is assumed about the initial morphology of the domain. This issue has received special attention over the past years since the publication of the papers by Bendsøe & Kikuchi [1] and Bendsøe [2]. The main advantage of this methodology is that the optimal topology can be obtained even from an initial configuration that is far away from the optimal one. For an overview of the area of topology optimization of continuum structures, the reader is referred to the review paper by Eschenauer & Olhoff [5], where 425 references are included.

Important contributions in the field of topology optimization have been obtained by characterizing the topology as a material density to be determined. In these methodologies the cavities correspond to a region of zero density while the domain is identified by the region where the density is non-zero. This approach is based in the concepts of relaxed formulations and homogenization techniques (see, for instance, Bendsøe & Kikuchi [1]), where, in order to obtain different densities throughout the domain, a class of microcells of laminated material is introduced and an homogenization method is used to

compute the physical properties of these microstructures. Therefore, the optimal solution may be seen as a distribution of fictitious materials that compose the domain. Finally, penalization methods and filtering techniques are needed to retrieve the feasible design.

More recently, Eschenauer et al. [6], Schumacher [16], Céa et al. [4], Garreau et al. [9, 10] and Sokolowski & Żochowski [18, 19] presented a method to obtain the optimal topology by calculating the so-called Topological Derivative. This derivative is a function defined in the domain of interest where, at each point, it gives the sensitivity of the cost function when a small hole is created at that point, Fig. (1). Following the paper by Eschenauer & Olhoff [5], the Topological Derivative concept has been used to solve topology optimization problems where no restrictions concerning the nature of the phenomena as well as the boundary conditions imposed on the holes are made. However, according to the approach adopted in the referenced works, this quite general concept can become restrictive, due to mathematical difficulties involved in the calculation of the Topological Derivative. In fact, the work of Garreau et al. [10] introduced several simplification hypothesis. For example, the cost function was assumed to be independent of the domain, only homogeneous Dirichlet and Neumann boundary conditions on the holes were considered, the source terms of the boundary value problem were assumed to be constant.

On the other hand, Shape Sensitivity Analysis, which has been shown to be a powerful tool to solve shape optimization problems, was proposed by Sokolowski & Żochowski [18] and Céa et al. [4] as an alternative way to evaluate the Topological Derivative. Nevertheless, their theory yields correct results only for some particular cases (for example, homogeneous Neumann boundary conditions on the hole). Moreover, in these works, the relation between both concepts was stated without mathematical proof, remaining open up to the present work.

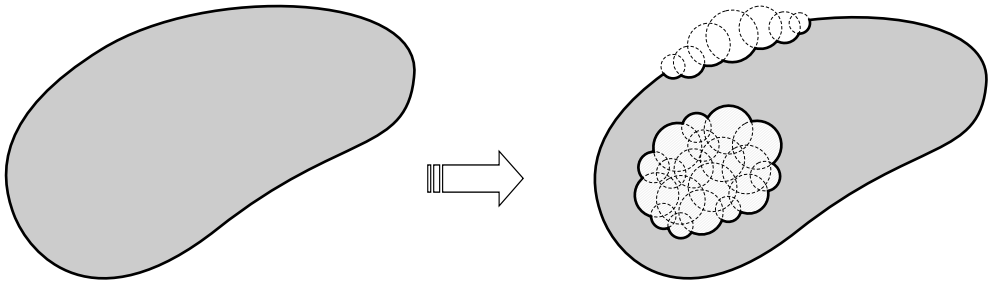

Figure 1: Obtaining the optimal topology via Topological Derivative.

In this work is introduced a novel definition for the Topological Derivative which allows to correctly use results from Shape Sensitivity Analysis. This new approach, from now on denoted *Topological-Shape Sensitivity Analysis*, is presented in Theorem 1, which formally establishes the relation between both concepts (Topological Derivative and Shape Sensitivity Analysis). Moreover, since Shape Sensitivity Analysis theory is well developed and has a strong mathematical foundation, this new methodology leads to a simple and constructive procedure to calculate the Topological Derivative, that can be applied for a large class of linear and non-linear engineering problems.

Therefore, the goal of this paper is to present an alternative way to calculate the Topological Derivative based on the Shape Sensitivity Analysis concepts. Thus, for a review of the contributions in Topological Derivative, as well as how it is inserted in the context of topology optimization methods, the reader is referred to [5].

With these ideas in mind, the Topological-Shape Sensitivity Analysis will be presented in Sections 2-4 in the context of a general elliptic boundary value problem. Following this new approach, in Section 5 the Topological Derivative will be calculated for the Poisson's problem taking into account different boundary conditions on the holes (Dirichlet, Neumann or Robin). Finally, in Section 6, this derivative will be applied in some design problems of steady-state heat conduction.

2 Definition of the Topological Derivative

As already mentioned, the Topological Derivative furnishes for any point of the domain the sensitivity of the problem in creating a small hole in that point. Mathematically, this problem may be written in the following manner:

Let $\Omega \subset \mathbb{R}^2$ be an open bounded domain, whose boundary Γ is smooth enough, *i.e.* a unit normal vector $\mathbf{n}$ exist almost everywhere (a.e.), except possibly in a finite set of null measure. Let still $\Omega_\epsilon \subset \mathbb{R}^2$ be a new domain, such that $\Omega_\epsilon = \Omega - \overline{B}_\epsilon$, whose boundary is denoted by $\Gamma_\epsilon = \Gamma \cup \partial B_\epsilon$, where $\overline{B}_\epsilon = B_\epsilon \cup \partial B_\epsilon$ is a ball of radius ϵ centered on the point $\hat{\mathbf{x}} \in \Omega$. So, one has the original domain without hole Ω and the new one Ω_ϵ with a small hole $\overline{B}_\epsilon$, as may be seen in Fig. (2). Considering a cost function $\psi(\cdot)$ defined in a certain domain, then the Topological Derivative is written as (Garreau et al. [10])

$$D_T^*(\hat{\mathbf{x}}) := \lim_{\epsilon \to 0} \frac{\psi(\Omega_\epsilon) - \psi(\Omega)}{f(\epsilon)} , \tag{1}$$

where $f(\epsilon)$ is a negative function that decreases monotonically so that $f(\epsilon) \to 0$ with $\epsilon \to 0$ $(0 \leq \epsilon < 1)$, depending on the problem under analysis.

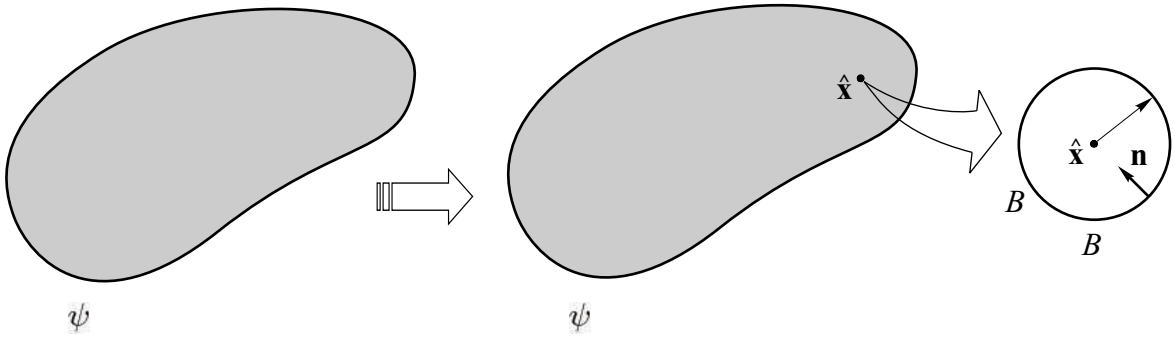

Figure 2: Original Topological Derivative concept.

The inconvenience of working with the definition given by Eq. (1) is that when a hole is created, it is impossible to establish an homeomorphism between the domains Ω_ϵ and Ω. So, the derivative (Eq. 1) cannot be obtained in a conventional way.

Therefore, the central idea of this work is to start from a problem in that the hole $\overline{B}_\epsilon$ already exists, *i.e.* from Ω_ϵ, causing a small perturbation $\delta\epsilon$ in the $\overline{B}_\epsilon$, so that the hole $\overline{B}_{\epsilon+\delta\epsilon}$ is originated, which is defined in a new domain $\Omega_{\epsilon+\delta\epsilon} = \Omega - \overline{B}_{\epsilon+\delta\epsilon}$, whose boundary is written as $\Gamma_{\epsilon+\delta\epsilon} = \Gamma \cup \partial B_{\epsilon+\delta\epsilon}$ (see Fig. 3). Thus, it shall be demonstrated that the Topological Derivative can be redefined in the following way:

$$D_T(\hat{\mathbf{x}}) := \lim_{\epsilon \to 0} \left\{ \lim_{\delta\epsilon \to 0} \frac{\psi(\Omega_{\epsilon+\delta\epsilon}) - \psi(\Omega_\epsilon)}{f(\epsilon+\delta\epsilon) - f(\epsilon)} \right\} = \lim_{\substack{\epsilon \to 0 \\ \delta\epsilon \to 0}} \frac{\psi(\Omega_{\epsilon+\delta\epsilon}) - \psi(\Omega_\epsilon)}{f(\epsilon+\delta\epsilon) - f(\epsilon)} . \tag{2}$$

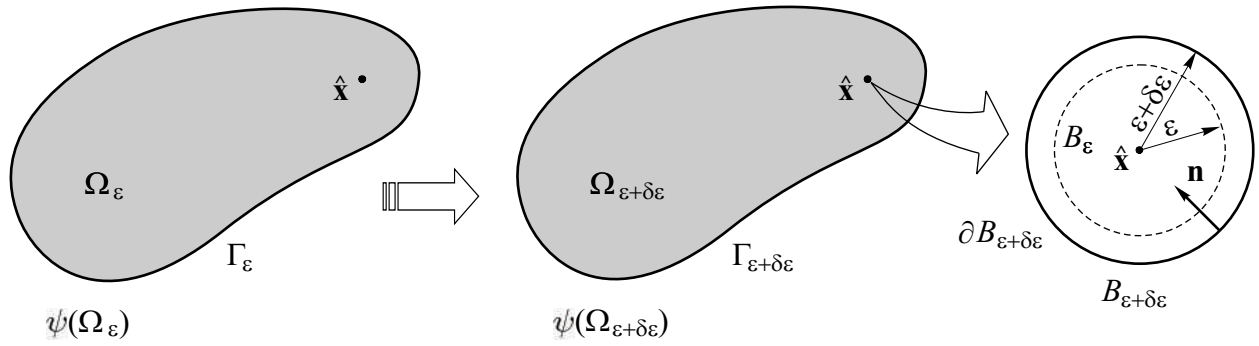

Figure 3: Modified Topological Derivative concept.

This last definition of the Topological Derivative (Eq. 2) merely provides the sensitivity of the problem when the size of the hole $\overline{B}_\epsilon$, with $\epsilon \to 0$, increases and not when it is effectively created (as one has in the original definition of the Topological Derivative given by Eq. 1). However, it is understood that to expand a hole of radius ϵ, when $\epsilon \to 0$, is nothing more than creating it. In fact, a complete mathematical proof that establishes the relation between both definitions given by Eqs. (1,2) shall be stated in Section 4 of the present work, where it is also shown that these equations are equivalent to Eq. (16). This last expression provides the formal relation between the Topological Derivative and the Shape Sensitivity Analysis. The advantage of the novel definition for the Topological Derivative given by Eq. (16) is that the whole mathematical framework developed for the Shape Sensitivity Analysis can be used, from now on, to compute the Topological Derivative.

3 Shape Sensitivity Analysis

Boundary value problems are formulated by differential equations defined point to point in the domain Ω or, in a more general form, by integral equations in Ω. Therefore, perturbations in this domain produce, necessarily, alterations as much in the integrand terms, as well as in the domain of integration itself. In this way, the Shape Sensitivity Analysis is nothing more than determining the variation of the characteristics associated to the problem due to the modifications in the configuration denoted by Ω. For such, one can use the concepts developed in the pioneering work of Murat & Simon [14], that is:

Let $\Omega_\epsilon \subset \mathbb{R}^2$ be the domain such as defined in Section 2. Considering that this domain suffers a perturbation, which can be represented by a smooth and invertible mapping dependent on the parameter τ, denoted by $\chi(\mathbf{x}, \tau)$ with $\mathbf{x} \in \Omega_\epsilon$ and $\tau \in \mathbb{R}$, then, the perturbed domain Ω_τ as well as its boundary Γ_τ, can be described, respectively, as

$$\begin{aligned} \Omega_\tau &:= \left\{ \mathbf{x}_\tau \in \mathbb{R}^2 \mid \exists\, \mathbf{x} \in \Omega_\epsilon, \quad \mathbf{x}_\tau = \chi(\mathbf{x}, \tau), \quad \mathbf{x}_0 = \mathbf{x} \quad \text{and} \quad \Omega_0 = \Omega_\epsilon \right\} , \\ \Gamma_\tau &:= \left\{ \mathbf{x}_\tau \in \mathbb{R}^2 \mid \exists\, \mathbf{x} \in \Gamma_\epsilon, \quad \mathbf{x}_\tau = \chi(\mathbf{x}, \tau), \quad \mathbf{x}_0 = \mathbf{x} \quad \text{and} \quad \Gamma_0 = \Gamma_\epsilon \right\} . \end{aligned}$$

Expanding $\chi(\mathbf{x}, \tau)$ in a Taylor series around $\tau_0 = 0$, one has that every point $\mathbf{x}_\tau$ may be written, for τ small enough, in the following manner

$$\mathbf{x}_\tau = \mathbf{x} + \tau \mathbf{V}(\mathbf{x}) \ , \tag{3}$$

where $\mathbf{V}(\mathbf{x})$ is the *shape change velocity* or, making a parallel with Continuum Mechanics (Gurtin [11]), it can be seen as the *material velocity*.

Thus, taking into account the Shape Sensitivity Analysis concepts, one need to establish the sensitivity of the cost function $\psi(\Omega_\tau)$ in relation to the perturbation characterized by τ, which is

given by the following derivative

$$\left.\frac{d\psi\left(\Omega_\tau\right)}{d\tau}\right|_{\tau=0} = \lim_{\tau\to 0}\frac{\psi\left(\Omega_\tau\right)-\psi(\Omega_0)}{\tau}\ . \tag{4}$$

In a quite general manner, the cost function $\psi\left(\Omega_\tau\right)$ can be defined in the following way (see, for instance, Fancello [8]):

$$\psi\left(\Omega_\tau\right) := \Psi_\tau\left(u_\tau\right) = \int_{\Omega_\tau}\phi_\Omega\left(u_\tau\right)\ d\Omega_\tau + \int_{\Gamma_\tau}\phi_\Gamma\left(u_\tau\right)\ d\Gamma_\tau\ , \tag{5}$$

where u_τ is an implicit function of τ through the boundary value problem described in the perturbed configuration Ω_τ, that is:

Find $u_\tau \in U_\tau$, such that

$$a_\tau\left(u_\tau, w_\tau\right) = l_\tau(w_\tau) \qquad \forall\ w_\tau \in V_\tau \text{ and } \forall\tau \geq 0\ . \tag{6}$$

where U_τ is the admissible functions set and V_τ is the admissible variations space, which will be defined later, according to the problem under analysis, and the operator $a_\tau\left(\cdot,\cdot\right) : U_\tau \times V_\tau \to \mathbb{R}$ is a continuous and V_τ-Elliptic bilinear form and $l_\tau\left(\cdot\right) : V_\tau \to \mathbb{R}$ is a continuous linear functional. In order to facilitate the presentation of this work, the operator $a_\tau\left(\cdot,\cdot\right)$ shall be considered symmetric.

Therefore, the derivative of $\Psi_\tau\left(u_\tau\right)$ in relation to the parameter τ at $\tau = 0$ is given by

$$\left.\frac{d}{d\tau}\Psi_\tau\left(u_\tau\right)\right|_{\tau=0} = \lim_{\tau\to 0}\frac{\Psi_\tau\left(u_\tau\right)-\Psi_0\left(u_0\right)}{\tau}\ . \tag{7}$$

where $u_0 = u_\tau|_{\tau=0} = u_\epsilon$ is the solution associated to the domain Ω_ϵ.

Formally, the calculation of this derivative (Eq. 7) can be written in the following way:

$$\left\{\begin{array}{ll} \textbf{Calculate :} & \dfrac{d}{d\tau}\ \Psi_\tau\left(u_\tau\right)|_{\tau=0} \\ \textbf{Subject to :} & a_\tau\left(u_\tau, w_\tau\right) = l_\tau(w_\tau) \quad \forall\ w_\tau \in V_\tau \text{ and } \forall\tau \geq 0 \end{array}\right. . \tag{8}$$

This issue can be realized using the Lagrangian Method that consists in relaxing the constraint of the problem, in this case the state equation (Eq. 6), by the Lagrangian multipliers. Therefore, the Lagrangian written already in the perturbed configuration Ω_τ

$$\pounds_\tau\left(u_\tau, \lambda_\tau\right) = \Psi_\tau\left(u_\tau\right) + a_\tau\left(u_\tau, \lambda_\tau\right) - l_\tau\left(\lambda_\tau\right) \quad \forall\lambda_\tau \in V_\tau\ , \tag{9}$$

allows the derivation of the Shape Sensitivity of the cost function in the following way:

$$\frac{d}{d\tau}\Psi_\tau\left(u_\tau\right) = \frac{\partial}{\partial\tau}\pounds_\tau\left(u_\tau, \lambda_\tau\right) = \frac{\partial}{\partial\tau}\Psi_\tau\left(u_\tau\right) + \frac{\partial}{\partial\tau}a_\tau\left(u_\tau, \lambda_\tau\right) - \frac{\partial}{\partial\tau}l_\tau\left(\lambda_\tau\right)\ , \tag{10}$$

where $u_\tau \in U_\tau$ is the solution of the state problem (Eq. 6) and $\lambda_\tau \in V_\tau$ is the solution of the *adjoint equation* given by

$$a_\tau\left(\lambda_\tau, w_\tau\right) = -\left\langle\frac{\partial\Psi_\tau}{\partial u_\tau}, w_\tau\right\rangle \qquad \forall \quad w_\tau \in V_\tau\ . \tag{11}$$

Finally, it is enough to show how the Shape Sensitivity Analysis concepts can be utilized to obtain the Topological Derivative $D_T\left(\hat{\mathbf{x}}\right)$, given by the Eqs. (1 or 2), linking, thereafter, both concepts.

4 Topological-Shape Sensitivity Analysis

Let $\psi(\cdot)$ be a cost function defined in the domains $\Omega_\epsilon = \Omega - \overline{B}_\epsilon$ and $\Omega_{\epsilon+\delta\epsilon} = \Omega - \overline{B}_{\epsilon+\delta\epsilon}$. Considering the Shape Sensitivity Analysis concepts presented earlier in Section 3, one has

$$\Omega_{\epsilon+\delta\epsilon} = \Omega_\tau \Rightarrow \Omega_\epsilon = \Omega_0 \quad \text{and} \quad \Gamma_{\epsilon+\delta\epsilon} = \Gamma_\tau \Rightarrow \Gamma_\epsilon = \Gamma_0 \ , \tag{12}$$

remembering that only the ball $\overline{B}_\epsilon$ suffers a perturbation $\delta\epsilon$.

A well-known result (see, for instance, Zolésio [23]), is that only the velocity component in the normal direction to boundary Γ_ϵ is significant in the calculation of sensitivity. This result is based on the idea that only this component, that is V_n, effectively produces change in the shape of the body. Therefore, considering that $\mathbf{V}$ defines an *action of change of form* such as indicated in Fig. (3), then this velocity field may be defined as

$$\left\{ \begin{array}{ll} \mathbf{V} = V_n \mathbf{n} & \text{with } V_n < 0 \text{ constant on } \partial B_\epsilon \\ \mathbf{V} = \mathbf{0} & \text{on } \Gamma, \text{ remembering that } \Gamma_\epsilon = \Gamma \cup \partial B_\epsilon \end{array} \right. . \tag{13}$$

Therefore, the Eq. (3) results in

$$\mathbf{x}_\tau = \mathbf{x} + \tau V_n \mathbf{n}, \quad \forall \mathbf{x} \in \partial B_\epsilon \ . \tag{14}$$

In this way, it is possible to associate the perturbation $\delta\epsilon$ with the parameter τ, that is, from the Eqs. (12,14) and observing that $\delta\epsilon = \|\mathbf{x}_\tau - \mathbf{x}\|$ for $\mathbf{x} \in \partial B_\epsilon$ and $\mathbf{x}_\tau \in \partial B_{\epsilon+\delta\epsilon}$, one has that

$$\delta\epsilon = \|\tau V_n \mathbf{n}\| = \tau \left| V_n \right| \ . \tag{15}$$

Now, the relation between the Topological Derivative and the Shape Sensitivity Analysis concepts can be demonstrated in the following theorem:

Theorem 1 (Topological-Shape Sensitivity Analysis) *Let $f(\epsilon)$ be a function chosen in order to $0 < |D_T^*(\hat{\mathbf{x}})| < \infty$, then the limit with $\epsilon \to 0$ that appears in the definition of the Topological Derivative given by Eq. (1) can be written as*

$$D_T^*(\hat{\mathbf{x}}) = D_T(\hat{\mathbf{x}}) = \lim_{\epsilon \to 0} \frac{1}{f'(\epsilon)\left|V_n\right|} \frac{d\psi(\Omega_\tau)}{d\tau}\bigg|_{\tau=0} \ . \tag{16}$$

Proof. *The proof of this theorem is divided into two parts*

$$\textbf{\textit{Part 1}}: D_T(\hat{\mathbf{x}}) = D_T^*(\hat{\mathbf{x}}) \ , \tag{17}$$

$$\textbf{\textit{Part 2}}: D_T(\hat{\mathbf{x}}) = \lim_{\epsilon \to 0} \frac{1}{f'(\epsilon)\left|V_n\right|} \frac{d\psi(\Omega_\tau)}{d\tau}\bigg|_{\tau=0} \ . \tag{18}$$

Proof of Part 1: *From the Eq. (1) one has that*

$$\psi(\Omega_\epsilon) = \psi(\Omega) + D_T^*(\hat{\mathbf{x}}) f(\epsilon) + \mathcal{R}(f(\epsilon)) \ , \tag{19}$$

where $\mathcal{R}(f(\epsilon))$ is used to indicate the higher order terms than $f(\epsilon)$, that is

$$\lim_{\epsilon \to 0} \frac{\mathcal{R}(f(\epsilon))}{f(\epsilon)} = 0 \ .$$

In the same way, one has that

$$\psi(\Omega_{\epsilon+\delta\epsilon}) = \psi(\Omega) + D_T^*(\hat{\mathbf{x}}) f(\epsilon+\delta\epsilon) + \mathcal{R}(f(\epsilon+\delta\epsilon)) \ . \tag{20}$$

Subtracting the Eq. (19) from the Eq. (20) comes

$$\psi(\Omega_{\epsilon+\delta\epsilon}) - \psi(\Omega_\epsilon) = D_T^*(\hat{\mathbf{x}}) \left(f(\epsilon + \delta\epsilon) - f(\epsilon) \right) + \mathcal{R}\left(f\left(\epsilon + \delta\epsilon\right)\right) - \mathcal{R}\left(f\left(\epsilon\right)\right) \ . \tag{21}$$

Dividing the Eq. (21) by $f\left(\epsilon + \delta\epsilon\right) - f\left(\epsilon\right)$ *one obtains*

$$\frac{\psi(\Omega_{\epsilon+\delta\epsilon}) - \psi(\Omega_\epsilon)}{f(\epsilon + \delta\epsilon) - f(\epsilon)} = D_T^*(\hat{\mathbf{x}}) + \frac{\mathcal{R}\left(f\left(\epsilon + \delta\epsilon\right)\right) - \mathcal{R}\left(f\left(\epsilon\right)\right)}{f\left(\epsilon + \delta\epsilon\right) - f\left(\epsilon\right)} \ .$$

Taking the limits as indicated in the Eq. (2), one has

$$D_T(\hat{\mathbf{x}}) = \lim_{\substack{\epsilon\to 0 \\ \delta\epsilon\to 0}} \frac{\psi\left(\Omega_{\epsilon+\delta\epsilon}\right) - \psi(\Omega_\epsilon)}{f\left(\epsilon + \delta\epsilon\right) - f\left(\epsilon\right)} = D_T^*(\hat{\mathbf{x}}) + \lim_{\substack{\epsilon\to 0 \\ \delta\epsilon\to 0}} \frac{\mathcal{R}\left(f\left(\epsilon + \delta\epsilon\right)\right) - \mathcal{R}\left(f\left(\epsilon\right)\right)}{f\left(\epsilon + \delta\epsilon\right) - f\left(\epsilon\right)} \ . \tag{22}$$

Applying the L'Hopital theorem

$$\lim_{\substack{\epsilon\to 0 \\ \delta\epsilon\to 0}} \frac{\mathcal{R}\left(f\left(\epsilon + \delta\epsilon\right)\right) - \mathcal{R}\left(f\left(\epsilon\right)\right)}{f\left(\epsilon + \delta\epsilon\right) - f\left(\epsilon\right)} = \lim_{\substack{\epsilon\to 0 \\ \delta\epsilon\to 0}} \mathcal{R}'\left(f\left(\epsilon + \delta\epsilon\right)\right) = 0$$

and substituting this last result in the Eq. (22), one obtains the proof of the first part of this theorem, that is,

$$D_T\left(\hat{\mathbf{x}}\right) = D_T^*\left(\hat{\mathbf{x}}\right) \ .$$

Proof of Part 2: *Let be the Eq. (2), which can be written as*

$$D_T\left(\hat{\mathbf{x}}\right) = \lim_{\substack{\epsilon\to 0 \\ \delta\epsilon\to 0}} \frac{\psi\left(\Omega_{\epsilon+\delta\epsilon}\right) - \psi(\Omega_\epsilon)}{\frac{f(\epsilon+\delta\epsilon)-f(\epsilon)}{\delta\epsilon}\delta\epsilon} \ . \tag{23}$$

But one can observe that

$$\lim_{\delta\epsilon\to 0} \frac{f\left(\epsilon + \delta\epsilon\right) - f\left(\epsilon\right)}{\delta\epsilon} = f'\left(\epsilon\right) \ . \tag{24}$$

Substituting the Eq. (24) in the Eq. (23) comes

$$D_T\left(\hat{\mathbf{x}}\right) = \lim_{\epsilon\to 0} \frac{1}{f'\left(\epsilon\right)} \lim_{\delta\epsilon\to 0} \frac{\psi\left(\Omega_{\epsilon+\delta\epsilon}\right) - \psi(\Omega_\epsilon)}{\delta\epsilon} \ . \tag{25}$$

Considering the Eqs. (12,4), the Eq. (25) can be written, taking into account that $\delta\epsilon = \tau\left|V_n\right|$ *(Eq. 15), in the following manner*

$$D_T\left(\hat{\mathbf{x}}\right) = \lim_{\epsilon\to 0} \frac{1}{f'\left(\epsilon\right)} \lim_{\tau\to 0} \frac{\psi\left(\Omega_\tau\right) - \psi(\Omega_0)}{\tau\left|V_n\right|} = \lim_{\epsilon\to 0} \frac{1}{f'\left(\epsilon\right)\left|V_n\right|} \left.\frac{d\psi\left(\Omega_\tau\right)}{d\tau}\right|_{\tau=0} \ . \tag{26}$$

Finally, from the Eq. (26) and the result of the first part of this demonstration (Eq. 17), one can verify that

$$D_T^*\left(\hat{\mathbf{x}}\right) = D_T\left(\hat{\mathbf{x}}\right) = \lim_{\epsilon\to 0} \frac{1}{f'\left(\epsilon\right)\left|V_n\right|} \left.\frac{d\psi\left(\Omega_\tau\right)}{d\tau}\right|_{\tau=0}$$

and the theorem is demonstrated ■

This fundamental result establishes, formally, the relation between the Topological Derivative and the Shape Sensitivity Analysis concepts, such as Sokolowski & Żochowski [18] and Céa et al. [4] have been perceived.

5 Topological Derivative applied to the Poisson's problems

To illustrate the potentialities of the result of Theorem 1, the Topological Derivative will be calculated, utilizing the Eq. (16), in the problem of steady-state energy transfer in two-dimensional[1] rigid bodies. From the equations of the first law of the thermodynamics (energy balance) in permanent regime and considering the constitutive equation given by the Fourier's law for isotropic materials, one has a problem that may be modeled by a second order elliptic boundary value problem, classically known as the Poisson's equation (see, for instance, Carlson [3] or Slattery [17]). On the holes, boundary conditions will be imposed either in the temperature (Dirichlet), in the heat flux (Neumann) or even in both variables (Robin). Physically, the holes can be interpreted as cooling channels, where the convection is totally predominant (prescribed temperature) or where there is a prescribed heat flux (thermal isolation, for example). A more realistic situation can be considered admitting a finite and non-null convection in the holes. Such a phenomenon can be modeled through the well-known Newton's law of cooling, leading to the mixed boundary conditions (Robin) on the holes.

5.1 Formulation of the problem

Let a rigid body be represented by $\Omega_\epsilon \subset \mathbb{R}^2$ with a small hole $\overline{B}_\epsilon$ centered in $\hat{\mathbf{x}} \in \Omega$, whose boundary $\Gamma_\epsilon = \Gamma \cup \partial B_\epsilon$ is such that $\Gamma = \Gamma_N \cup \Gamma_D \cup \Gamma_R$, with Γ_N, Γ_D, Γ_R, ∂B_ϵ mutually disjoint. Considering that the body is submitted to a constant excitation b in the domain Ω_ϵ and Dirichlet (or essential), Neumann (or natural) and/or Robin (or mixed) boundary conditions on Γ_D, Γ_N and Γ_R, respectively, and that on the contour of the holes (on ∂B_ϵ), will also be imposed either Dirichlet, Neumann or Robin boundary conditions. Thus, the solution u_ϵ must satisfy the Poisson's equation, that is:

$$\left\{\begin{array}{lll} \text{Find } u_\epsilon, \text{ such that} & & \\ -k\Delta u_\epsilon = b & \text{in} & \Omega_\epsilon \\ u_\epsilon = \bar{u} & \text{on} & \Gamma_D \\ -k\dfrac{\partial u_\epsilon}{\partial n} = \bar{q} & \text{on} & \Gamma_N \\ -k\dfrac{\partial u_\epsilon}{\partial n} = h_c\,(u_\epsilon - u_\infty) & \text{on} & \Gamma_R \\ h(\alpha,\beta,\gamma) = 0 & \text{on} & \partial B_\epsilon \end{array}\right. , \tag{27}$$

where the function $h(\alpha,\beta,\gamma)$ is such that:

$$h(\alpha,\beta,\gamma) = \alpha\,(u_\epsilon - \bar{u}^\epsilon) + \beta\left(k\frac{\partial u_\epsilon}{\partial n} + \bar{q}^\epsilon\right) + \gamma\left(k\frac{\partial u_\epsilon}{\partial n} + h_c^\epsilon\,(u_\epsilon - u_\infty^\epsilon)\right) = 0\,, \tag{28}$$

and $\alpha,\beta,\gamma \in \{0,1\}$ with $\alpha+\beta+\gamma = 1$.

Therefore, the three kind of boundary conditions on ∂B_ϵ considered in this work are obtained combining the parameters α, β and γ adequately, that is:

$$h(\alpha,\beta,\gamma) = \left\{\begin{array}{lll} u_\epsilon - \bar{u}^\epsilon, & \text{if } \alpha=1, \beta=\gamma=0, & \text{Dirichlet} \\ k\dfrac{\partial u_\epsilon}{\partial n} + \bar{q}^\epsilon, & \text{if } \beta=1, \alpha=\gamma=0, & \text{Neumann} \\ k\dfrac{\partial u_\epsilon}{\partial n} + h_c^\epsilon\,(u_\epsilon - u_\infty^\epsilon)\,, & \text{if } \gamma=1, \alpha=\beta=0, & \text{Robin} \end{array}\right. . \tag{29}$$

The parameters k, $\bar{u}$, $\bar{q}$, u_∞, h_c, $\bar{u}^\epsilon$, $\bar{q}^\epsilon$, u_∞^ϵ and h_c^ϵ are considered, for simplicity, constants in relation to τ, where:

- k is the thermal conductivity;

[1] It is important to mention that the extension to three-dimensional domains is straightforward to consider.

- $\bar{u}$ is the prescribed temperature on Γ_D;

- $\bar{q}$ is the prescribed heat flux on Γ_N;

- u_∞ and h_c are the temperature and the heat-transfer coefficient of the outside medium, respectively;

- $\bar{u}^\epsilon$ is the prescribed temperature on ∂B_ϵ, when $\alpha = 1, \beta = \gamma = 0$;

- $\bar{q}^\epsilon$ is the prescribed heat flux on ∂B_ϵ, when $\beta = 1, \alpha = \gamma = 0$;

- u_∞^ϵ and h_c^ϵ are the temperature and the heat-transfer coefficient in the interior of the channels, respectively, when $\gamma = 1, \alpha = \beta = 0$;

The problem given by Eq. (27) can be written in the variational form. In other words, this means to solve the set of Eqs. (27) in the weak sense, that is:

Find $u_\epsilon \in U_\epsilon$, such that

$$a_\epsilon\left(u_\epsilon, w_\epsilon\right) = l_\epsilon\left(w_\epsilon\right) \qquad \forall\ w_\epsilon \in V_\epsilon\ , \tag{30}$$

where $a_\epsilon\left(u_\epsilon, w_\epsilon\right)$ and $l_\epsilon\left(w_\epsilon\right)$ are written, respectively, as

$$a_\epsilon\left(u_\epsilon, w_\epsilon\right) = \int_{\Omega_\epsilon} k\nabla u_\epsilon \cdot \nabla w_\epsilon\ d\Omega_\epsilon + \int_{\Gamma_R} h_c u_\epsilon w_\epsilon\ d\Gamma + \gamma \int_{\partial B_\epsilon} h_c^\epsilon u_\epsilon w_\epsilon\ d\partial B_\epsilon\ , \tag{31}$$

$$\begin{aligned} l_\epsilon\left(w_\epsilon\right) = & \int_{\Omega_\epsilon} b w_\epsilon\ d\Omega_\epsilon - \int_{\Gamma_N} \bar{q} w_\epsilon\ d\Gamma + \int_{\Gamma_R} h_c u_\infty w_\epsilon\ d\Gamma \\ & - \beta \int_{\partial B_\epsilon} \bar{q}^\epsilon w_\epsilon\ d\partial B_\epsilon + \gamma \int_{\partial B_\epsilon} h_c^\epsilon u_\infty^\epsilon w_\epsilon\ d\partial B_\epsilon \end{aligned} \tag{32}$$

and the admissible functions set U_ϵ and the admissible variations space V_ϵ are given, respectively, by

$$\begin{aligned} U_\epsilon &= \left\{ u_\epsilon \in H^1\left(\Omega_\epsilon\right) \mid u_\epsilon|_{\Gamma_D} = \bar{u} \text{ and } \alpha\ u_\epsilon|_{\partial B_\epsilon} = \alpha \bar{u}^\epsilon \right\}\ , \\ V_\epsilon &= \left\{ w_\epsilon \in H^1\left(\Omega_\epsilon\right) \mid w_\epsilon|_{\Gamma_D} = 0 \text{ and } \alpha\ w_\epsilon|_{\partial B_\epsilon} = 0 \right\}\ , \end{aligned}$$

where $H^1\left(\cdot\right)$ is a Hilbert space of order 1 defined in a given domain. It is important to mention that, when $\alpha = 1,\ u_\epsilon|_{\partial B_\epsilon} = \bar{u}^\epsilon$ and $w_\epsilon|_{\partial B_\epsilon} = 0$; and when $\alpha = 0,\ u_\epsilon|_{\partial B_\epsilon}$ and $w_\epsilon|_{\partial B_\epsilon}$ are free on ∂B_ϵ.

As seen in Section 3, the boundary value problem written in the reference configuration (Eq. 30), must also be satisfied in the perturbed configuration Ω_τ, $\forall \tau \geq 0$. In this way, considering the Eq. (6), the bilinear form $a_\tau\left(u_\tau, w_\tau\right)$ and the linear functional $l_\tau\left(w_\tau\right)$ are given, respectively, by

$$a_\tau\left(u_\tau, w_\tau\right) = \int_{\Omega_\tau} k\nabla_\tau u_\tau \cdot \nabla_\tau w_\tau\ d\Omega_\tau + \int_{\Gamma_R} h_c u_\tau w_\tau\ d\Gamma + \gamma \int_{\partial B_{\epsilon_\tau}} h_c^\epsilon u_\tau w_\tau\ d\partial B_{\epsilon_\tau}\ , \tag{33}$$

$$\begin{aligned} l_\tau\left(w_\tau\right) = & \int_{\Omega_\tau} b w_\tau\ d\Omega_\tau - \int_{\Gamma_N} \bar{q} w_\tau\ d\Gamma + \int_{\Gamma_R} h_c u_\infty w_\tau\ d\Gamma \\ & - \beta \int_{\partial B_{\epsilon_\tau}} \bar{q}^\epsilon w_\tau\ d\partial B_{\epsilon_\tau} + \gamma \int_{\partial B_{\epsilon_\tau}} h_c^\epsilon u_\infty^\epsilon w_\tau\ d\partial B_{\epsilon_\tau}\ , \end{aligned} \tag{34}$$

where $u_\tau \in U_\tau := U_\epsilon(\Omega_\tau)$, $w_\tau \in V_\tau := V_\epsilon(\Omega_\tau)$, $\epsilon_\tau = \epsilon + \tau\left|V_n\right|$ and $\nabla_\tau\left(\cdot\right)$ is adopted to denote

$$\nabla_\tau\left(\cdot\right) := \frac{\partial}{\partial \mathbf{x}_\tau}\left(\cdot\right)\ .$$

Observe that the boundary $\Gamma = \Gamma_N \cup \Gamma_D \cup \Gamma_R$ is fixed, as can be seen in the definition of the velocity field given by Eq. (13).

5.2 Calculus of the Topological Derivative

To obtain the expression of the Topological-Shape Sensitivity Analysis, it is necessary firstly to calculate the derivative of the cost function $\Psi_\tau(u_\tau)$ in relation to the parameter τ, at $\tau = 0$ (see Theorem 1, Eq. 16). As seen in Section 3, the calculation of sensitivity of the cost function Ψ_τ can be realized evoking the Lagrangian Method, that is: Let u_τ and λ_τ be solutions of the state and adjoint equations, respectively, then Eq. (10) holds.

The cost function Ψ_τ is, in a certain way, arbitrary. However, to arrive at its derivative one must adopt a Ψ_τ in particular, depending on the interest and the application that one has in mind. In the heat conduction problem here under study it can be adopted, among others, cost functions like:

a - Internal energy

$$\Psi_\tau(u_\tau) := \frac{1}{2} a_\tau(u_\tau, u_\tau) \ . \tag{35}$$

b - Work of external sources (compliance)

$$\Psi_\tau(u_\tau) := l_\tau(u_\tau) \ . \tag{36}$$

c - Total potential energy

$$\Psi_\tau(u_\tau) := \frac{1}{2} a_\tau(u_\tau, u_\tau) - l_\tau(u_\tau) \ . \tag{37}$$

d - Energy in transit

$$\Psi_\tau(u_\tau) := \int_{\Omega_\tau} |\mathbf{q}_\tau|^2 \ d\Omega_\tau \ , \quad \text{where} \quad \mathbf{q}_\tau = -k\nabla_\tau u_\tau \ . \tag{38}$$

e - Prescribed temperature on a fixed portion $\Gamma_{\bar{u}}$ of the contour Γ_ϵ

$$\Psi(u_\tau) := \int_{\Gamma_{\bar{u}}} (u_\tau - \bar{u})^2 \ d\Gamma \ . \tag{39}$$

f - Prescribed flux on a fixed portion $\Gamma_{\bar{q}}$ of the contour Γ_ϵ

$$\Psi(u_\tau) := \int_{\Gamma_{\bar{q}}} \left(k\frac{\partial u_\tau}{\partial n} + \bar{q} \right)^2 \ d\Gamma \ . \tag{40}$$

For the linear problem here considered, the choice of whatever of the cost functions (a), (b) and (c) results equivalent and simplifies the calculation of the Topological Derivative because the solution λ_τ (Eq. 11) can be obtained explicitly, that is, without the necessity of solving the adjoint equation. This doesn't occur with the cost functions (d), (e) and (f), which require that the adjoint equation must be effectively solved, increasing, therefore, the computational cost of the problem.

Following, the total potential energy (cost function (c), Eq. 37) is adopted as an example of objective function, which, in this case, is defined as[2]:

$$\begin{aligned}\Psi_\tau(u_\tau) := \frac{1}{2}\Bigg(& \int_{\Omega_\tau} k\nabla_\tau u_\tau \cdot \nabla_\tau u_\tau \ d\Omega_\tau + \int_{\Gamma_R} h_c u_\tau^2 \ d\Gamma + \gamma \int_{\partial B_{\epsilon_\tau}} h_c^\epsilon u_\tau^2 \ d\partial B_{\epsilon_\tau} \Bigg) \\ & - \int_{\Omega_\tau} b u_\tau \ d\Omega_\tau + \int_{\Gamma_N} \bar{q} u_\tau \ d\Gamma - \int_{\Gamma_R} h_c u_\infty u_\tau \ d\Gamma \\ & + \beta \int_{\partial B_{\epsilon_\tau}} \bar{q}^\epsilon u_\tau \ d\partial B_{\epsilon_\tau} - \gamma \int_{\partial B_{\epsilon_\tau}} h_c^\epsilon u_\infty^\epsilon u_\tau \ d\partial B_{\epsilon_\tau} \ .\end{aligned} \tag{41}$$

[2] A physical interpretation for that function will be discussed in more detail in Section 6.

It is important to stand out that the methodology here proposed is not limited to this cost function in particular (Eq. 37), that is, any one of the six cost functions presented could be adopted, or another more general (even with constraints, for example) that haven't been mentioned.

Once characterized the cost function to be studied (Eq. 41), one can calculate the derivative of the Lagrangian (Eq. 10). Thus, the adjoint equation (Eq. 11) for this particular case remains:

Find $\lambda_\tau \in V_\tau$, such that

$$\begin{aligned} a_\tau\left(\lambda_\tau, w_\tau\right) &= -\left\langle \frac{\partial \Psi_\tau}{\partial u_\tau}, w_\tau \right\rangle \\ &= -\left(a_\tau\left(u_\tau, w_\tau\right) - l_\tau\left(w_\tau\right)\right) = 0 \qquad \forall\ w_\tau \in V_\tau\ , \\ &\Rightarrow \lambda_\tau = 0, \text{ see Eq. (6)}\ . \end{aligned} \tag{42}$$

Therefore, for u_τ and $\lambda_\tau = 0$ solutions of the state and adjoint equations, respectively, the derivative of the Lagrangian (Eq. 10) remains

$$\frac{\partial}{\partial \tau}\pounds_\tau\left(u_\tau, u_\tau\right) = \frac{1}{2}\frac{\partial}{\partial \tau}a_\tau\left(u_\tau, u_\tau\right) - \frac{\partial}{\partial \tau}l_\tau\left(u_\tau\right)\ . \tag{43}$$

The derivatives in the referential configuration $\Omega_\tau|_{\tau=0} = \Omega_\epsilon$ can be obtained by the Reynolds' transport theorem (see, for instance, Gurtin [11]). Thus, the derivative of the bilinear form $a_\tau\left(u_\tau, u_\tau\right)$ becomes

$$\begin{aligned} \left.\frac{\partial a_\tau}{\partial \tau}\right|_{\tau=0} &= \int_{\Omega_\epsilon}\left[\left.\frac{\partial}{\partial \tau}\left(k\nabla_\tau u_\tau \cdot \nabla_\tau u_\tau\right)\right|_{\tau=0} + k\nabla u_\epsilon \cdot \nabla u_\epsilon\ \mathrm{div}\mathbf{V}\right] d\Omega_\epsilon \\ &\quad + \gamma \int_{\partial B_\epsilon} h_c^\epsilon u_\epsilon^2\ \mathrm{div}_\Gamma \mathbf{V}\ d\partial B_\epsilon\ , \end{aligned} \tag{44}$$

where $\mathrm{div}_\Gamma \mathbf{V} = (\mathbf{I} - \mathbf{n}\otimes\mathbf{n}) \cdot \nabla \mathbf{V}$ is the superficial divergent of the velocity $\mathbf{V}$.

The derivative of the gradient of a scalar field that appears in the Eq. (44), is given by

$$\left.\frac{\partial}{\partial \tau}\left(\nabla_\tau u_\tau\right)\right|_{\tau=0} = -\left(\nabla \mathbf{V}\right)^T \nabla u_\epsilon\ . \tag{45}$$

Substituting this last result in the Eq. (44) one has that

$$\begin{aligned} \left.\frac{\partial a_\tau}{\partial \tau}\right|_{\tau=0} &= -\int_{\Omega_\epsilon}\left[\left(\nabla \mathbf{V}^T + \nabla \mathbf{V}\right) k\nabla u_\epsilon \cdot \nabla u_\epsilon - k\nabla u_\epsilon \cdot \nabla u_\epsilon\ \mathrm{div}\mathbf{V}\right] d\Omega_\epsilon \\ &\quad + \gamma \int_{\partial B_\epsilon} h_c^\epsilon u_\epsilon^2\ \mathrm{div}_\Gamma \mathbf{V}\ d\partial B_\epsilon\ . \end{aligned} \tag{46}$$

In the same way, the derivative of the functional $l_\tau\left(u_\tau\right)$ can be calculated in the following manner

$$\begin{aligned} \left.\frac{\partial l_\tau}{\partial \tau}\right|_{\tau=0} &= \int_{\Omega_\epsilon} b u_\epsilon\ \mathrm{div}\mathbf{V}\ d\Omega_\epsilon - \beta \int_{\partial B_\epsilon} \bar{q}^\epsilon u_\epsilon\ \mathrm{div}_\Gamma \mathbf{V}\ d\partial B_\epsilon \\ &\quad + \gamma \int_{\partial B_\epsilon} h_c^\epsilon u_\infty^\epsilon u_\epsilon\ \mathrm{div}_\Gamma \mathbf{V}\ d\partial B_\epsilon\ . \end{aligned} \tag{47}$$

Thus, substituting the Eqs. (46,47) in the Eq. (43), the derivative of the Lagrangian becomes

$$\begin{aligned} \left.\frac{\partial \pounds_\tau}{\partial \tau}\right|_{\tau=0} &= -\frac{1}{2}\int_{\Omega_\epsilon}\left[\left(\nabla \mathbf{V}^T + \nabla \mathbf{V}\right) k\nabla u_\epsilon \cdot \nabla u_\epsilon - k\nabla u_\epsilon \cdot \nabla u_\epsilon\ \mathrm{div}\mathbf{V}\right] d\Omega_\epsilon \\ &\quad + \frac{1}{2}\gamma \int_{\partial B_\epsilon} h_c^\epsilon u_\epsilon^2\ \mathrm{div}_\Gamma \mathbf{V}\ d\partial B_\epsilon - \int_{\Omega_\epsilon} b u_\epsilon\ \mathrm{div}\mathbf{V}\ d\Omega_\epsilon \\ &\quad + \beta \int_{\partial B_\epsilon} \bar{q}^\epsilon u_\epsilon\ \mathrm{div}_\Gamma \mathbf{V}\ d\partial B_\epsilon - \gamma \int_{\partial B_\epsilon} h_c^\epsilon u_\infty^\epsilon u_\epsilon\ \mathrm{div}_\Gamma \mathbf{V}\ d\partial B_\epsilon\ . \end{aligned} \tag{48}$$

Rearranging the Eq. (48) one has

$$\left.\frac{d\pounds_\tau}{d\tau}\right|_{\tau=0} = -\frac{1}{2}\int_{\Omega_\epsilon} \boldsymbol{\Sigma}\cdot\nabla\mathbf{V}\; d\Omega_\epsilon + \frac{1}{2}\int_{\partial B_\epsilon} \left[\gamma h_c^\epsilon u_\epsilon\left(u_\epsilon - 2u_\infty^\epsilon\right) + 2\beta\bar{q}^\epsilon u_\epsilon\right]\; \mathrm{div}_\Gamma\mathbf{V}\; d\partial B_\epsilon\;, \tag{49}$$

where $\boldsymbol{\Sigma}$ can be interpreted as a generalization of the Energy-Momentum Tensor of Eshelby (see, for instance, Eshelby [7] or Taroco et al. [21]), which, for the problem under study, results in a second order symmetric tensor, given by

$$\boldsymbol{\Sigma} = 2\left(k\nabla u_\epsilon\otimes\nabla u_\epsilon\right) + \left(2bu_\epsilon - k\nabla u_\epsilon\cdot\nabla u_\epsilon\right)\mathbf{I}\;.$$

In the Eq. (49), the integral in the domain Ω_ϵ can be carry to the contour Γ_ϵ, that is, considering the tensorial relationship

$$\begin{aligned}\mathrm{div}\left(\boldsymbol{\Sigma}^T\mathbf{V}\right) &= \boldsymbol{\Sigma}\cdot\nabla\mathbf{V} + \mathbf{V}\cdot\mathrm{div}\boldsymbol{\Sigma}\;,\\ \boldsymbol{\Sigma}\cdot\nabla\mathbf{V} &= \mathrm{div}\left(\boldsymbol{\Sigma}^T\mathbf{V}\right) - \mathbf{V}\cdot\mathrm{div}\boldsymbol{\Sigma}\;,\end{aligned}$$

however, one has that

$$\begin{aligned}\mathrm{div}\boldsymbol{\Sigma} &= 2\left[\nabla\left(\nabla u_\epsilon\right)\right]k\nabla u_\epsilon + 2\nabla u_\epsilon\,\mathrm{div}\left(k\nabla u_\epsilon\right) + 2b\nabla u_\epsilon - 2\left[\nabla\left(\nabla u_\epsilon\right)\right]^T k\nabla u_\epsilon\\ &= 2\nabla u_\epsilon\left(k\Delta u_\epsilon + b\right)\;.\end{aligned}$$

Thus, from the state equation given by Eq. (27) one has that $\mathrm{div}\boldsymbol{\Sigma} = \mathbf{0}$, therefore,

$$\boldsymbol{\Sigma}\cdot\nabla\mathbf{V} = \mathrm{div}\left(\boldsymbol{\Sigma}^T\mathbf{V}\right)\;. \tag{50}$$

Finally, from the Eq. (50) the derivative of the Lagrangian (Eq. 49) becomes an integral only defined on the boundary Γ_ϵ, that is,

$$\left.\frac{d\Psi_\tau}{d\tau}\right|_{\tau=0} = \left.\frac{\partial\pounds_\tau}{\partial\tau}\right|_{\tau=0} = -\frac{1}{2}\int_{\Gamma_\epsilon}\boldsymbol{\Sigma}\mathbf{n}\cdot\mathbf{V}\; d\Gamma_\epsilon + \frac{1}{2}\int_{\partial B_\epsilon}\left[\gamma h_c^\epsilon u_\epsilon\left(u_\epsilon - 2u_\infty^\epsilon\right) + 2\beta\bar{q}^\epsilon u_\epsilon\right]\;\mathrm{div}_\Gamma\mathbf{V}\; d\partial B_\epsilon\;.$$

From the definition of the velocity field given by the Eq. (13) and remembering that $\epsilon_\tau = \epsilon + \tau\left|V_n\right|$ and that $\Omega_\epsilon\subset\mathbb{R}^2$, on has

$$\begin{aligned}\left.\frac{d}{d\tau}\int_{\partial B_{\epsilon_\tau}} d\partial B_{\epsilon_\tau}\right|_{\tau=0} &= \left.\frac{d}{d\tau}\left[2\pi\left(\epsilon+\tau\left|V_n\right|\right)\right]\right|_{\tau=0} = 2\pi\left|V_n\right|\;,\\ &= \int_{\partial B_\epsilon}\mathrm{div}_\Gamma\mathbf{V}\; d\partial B_\epsilon = 2\pi\epsilon\;\mathrm{div}_\Gamma\mathbf{V}\\ &\Rightarrow \mathrm{div}_\Gamma\mathbf{V} = \frac{1}{\epsilon}\left|V_n\right|\;.\end{aligned} \tag{51}$$

Further, as the portion of the boundary $\Gamma_\epsilon = \Gamma\cup\partial B_\epsilon$ effectively submitted to the perturbation $\delta\epsilon$ (or $\tau\left|V_n\right|$) is ∂B_ϵ, then the derivative of the cost function results in

$$\left.\frac{d\Psi_\tau}{d\tau}\right|_{\tau=0} = -\frac{1}{2}V_n\int_{\partial B_\epsilon}\left\{\boldsymbol{\Sigma}\mathbf{n}\cdot\mathbf{n} - \frac{sign\left(V_n\right)}{\epsilon}\left[\gamma h_c^\epsilon u_\epsilon\left(u_\epsilon - 2u_\infty^\epsilon\right) + 2\beta\bar{q}^\epsilon u_\epsilon\right]\right\} d\partial B_\epsilon\;. \tag{52}$$

Substituting the Eq. (52) in the definition of the Topological Derivative obtained via Shape Sensitivity Analysis (Eq. 16) and considering that the hole is subject to an expansion ($sign\,(V_n) = -1$), one has that

$$D_T\,(\hat{\mathbf{x}}) = \frac{1}{2}\lim_{\epsilon\to 0}\frac{1}{f'\,(\epsilon)}\int_{\partial B_\epsilon}\left\{\boldsymbol{\Sigma}\mathbf{n}\cdot\mathbf{n} + \frac{1}{\epsilon}\left[\gamma h_c^\epsilon u_\epsilon\,(u_\epsilon - 2u_\infty^\epsilon) + 2\beta\bar{q}^\epsilon u_\epsilon\right]\right\} d\partial B_\epsilon\ . \tag{53}$$

As the gradient ∇u_ϵ defined in the contour ∂B_ϵ can be decomposed into a normal and tangential components, that is

$$(\nabla u_\epsilon\cdot\mathbf{n})\,\mathbf{n} := \frac{\partial u_\epsilon}{\partial n}\mathbf{n} \qquad \text{and} \qquad (\nabla u_\epsilon\cdot\mathbf{t})\,\mathbf{t} := \frac{\partial u_\epsilon}{\partial t}\mathbf{t}\ ,$$

the Eq. (53) can be written, considering still that

$$\boldsymbol{\Sigma}\mathbf{n}\cdot\mathbf{n} = 2k\left(\frac{\partial u_\epsilon}{\partial n}\right)^2 + 2bu_\epsilon - k\nabla u_\epsilon\cdot\nabla u_\epsilon\ ,$$

in the following way

$$D_T\,(\hat{\mathbf{x}}) = \frac{1}{2}\lim_{\epsilon\to 0}\frac{1}{f'\,(\epsilon)}\int_{\partial B_\epsilon}\left\{k\left(\frac{\partial u_\epsilon}{\partial n}\right)^2 - k\left(\frac{\partial u_\epsilon}{\partial t}\right)^2 + 2bu_\epsilon + \frac{1}{\epsilon}\left[\gamma h_c^\epsilon u_\epsilon\,(u_\epsilon - 2u_\infty^\epsilon) + 2\beta\bar{q}^\epsilon u_\epsilon\right]\right\} d\partial B_\epsilon\ . \tag{54}$$

Now, it is enough to calculate this limit with $\epsilon\to 0$ to obtain the final expression of the Topological Derivative.

5.3 Calculus of the limit with $\epsilon\to 0$

This point of the work deserves special attention, since that via Shape Sensitivity Analysis one obtains the Topological Derivative expressed in terms of a limit with $\epsilon\to 0$ (Eq. 54). To calculate this limit, one needs to explicitly know the behavior of the solution u_ϵ when $\epsilon\to 0$, as well as its normal and tangential derivatives. Thus, an Asymptotic Analysis of u_ϵ shall be performed for the problem here studied, that is:

Considering a boundary value problem such as the one described by the Eq. (27), but now defined in a ring $A = B_R - \overline{B}_\epsilon \subset \Omega_\epsilon \subset \mathbb{R}^2$, centered in $\hat{\mathbf{x}}\in\Omega$, where $R >> \epsilon$ is such that $R\to 0$, when $\epsilon\to 0$. This new problem can be formulated in the following way:

$$\left\{\begin{array}{l} \text{Find } v_\epsilon, \text{ such that} \\ \quad -\Delta v_\epsilon = \tilde{b} \qquad \text{in} \quad A \\ \quad v_\epsilon = \varphi \qquad\quad \text{on} \quad \partial B_R \\ \quad \tilde{\alpha}v_\epsilon + \tilde{\beta}\dfrac{\partial v_\epsilon}{\partial n} = \tilde{h} \quad \text{on} \quad \partial B_\epsilon \end{array}\right. , \tag{55}$$

where $\tilde{b} = b/k$, $\tilde{\alpha} = \alpha + \gamma h_c^\epsilon$, $\tilde{\beta} = k\,(\beta+\gamma)$ and $\tilde{h} = \alpha\bar{u}^\epsilon - \beta\bar{q}^\epsilon + \gamma h_c^\epsilon u_\infty^\epsilon$ (see Eq. 28). Moreover, $\varphi := u_\epsilon|_{\partial B_R}$, then $v_\epsilon = u_\epsilon|_A$, *i.e.* both problems given by the Eqs. (27,55) have the same solution in A. In this way, one can use the method of separation of variables to make a Fourier series expansion of v_ϵ, in order to obtain u_ϵ explicitly. That is, introducing the polar coordinate system (r,θ), the solution v_ϵ, as a function of r and θ, can be expressed for $\epsilon\le r\le R$ as follows

$$v_\epsilon\,(r,\theta) = \sum_{n=0}^{\infty}\left(v_n(r)\cos n\theta + \hat{v}_n(r)\sin n\theta\right)\ .$$

Utilizing the boundary conditions

$$\left(\tilde{\alpha}v_\epsilon + \tilde{\beta}\frac{\partial v_\epsilon}{\partial n}\right)\Big|_{\partial B_\epsilon} = \tilde{h} \quad \text{and} \quad v_\epsilon|_{\partial B_R} = \varphi = \sum_{n=0}^{\infty}\left(R^n\varphi_n\cos n\theta + R^n\hat{\varphi}_n\sin n\theta\right) \ ,$$

one obtains

$$\begin{aligned} v_\epsilon(r,\theta) = &-\frac{\tilde{b}}{4}r^2 + \ln r\left(\frac{\tilde{\alpha}\frac{\tilde{b}}{4}(R^2-\epsilon^2) + \tilde{\alpha}\varphi_0 - \tilde{h} + \tilde{\beta}\frac{\tilde{b}}{2}\epsilon}{\tilde{\alpha}(\ln R - \ln\epsilon) + \tilde{\beta}/\epsilon}\right) \\ &+ \frac{\ln R\left(\tilde{h} + \tilde{\alpha}\frac{\tilde{b}}{4}\epsilon^2 - \tilde{\beta}\frac{\tilde{b}}{2}\epsilon\right) - \left(\tilde{\alpha}\ln\epsilon - \tilde{\beta}/\epsilon\right)\left(\varphi_0 + \frac{\tilde{b}}{4}R^2\right)}{\tilde{\alpha}(\ln R - \ln\epsilon) + \tilde{\beta}/\epsilon} \\ &+ \sum_{n=1}^{\infty}\frac{\left(\epsilon\tilde{\alpha} + n\tilde{\beta}\right)r^n - \epsilon^{2n}\left(\epsilon\tilde{\alpha} - n\tilde{\beta}\right)r^{-n}}{\left(\epsilon\tilde{\alpha} + n\tilde{\beta}\right) - (\epsilon/R)^{2n}\left(\epsilon\tilde{\alpha} - n\tilde{\beta}\right)}\left(\varphi_n\cos n\theta + \hat{\varphi}_n\sin n\theta\right) \ . \end{aligned}$$

The solution $u_\epsilon|_{\partial B_\epsilon} = v_\epsilon|_{\partial B_\epsilon} = v_\epsilon(\epsilon,\theta)$ is easily calculated as

$$\begin{aligned} u_\epsilon|_{\partial B_\epsilon} = &-\frac{\tilde{b}}{4}\epsilon^2 + \ln\epsilon\left(\frac{\tilde{\alpha}\frac{\tilde{b}}{4}(R^2-\epsilon^2) + \tilde{\alpha}\varphi_0 - \tilde{h} + \tilde{\beta}\frac{\tilde{b}}{2}\epsilon}{\tilde{\alpha}(\ln R - \ln\epsilon) + \tilde{\beta}/\epsilon}\right) \\ &+ \frac{\ln R\left(\tilde{h} + \tilde{\alpha}\frac{\tilde{b}}{4}\epsilon^2 - \tilde{\beta}\frac{\tilde{b}}{2}\epsilon\right) - \left(\tilde{\alpha}\ln\epsilon - \tilde{\beta}/\epsilon\right)\left(\varphi_0 + \frac{\tilde{b}}{4}R^2\right)}{\tilde{\alpha}(\ln R - \ln\epsilon) + \tilde{\beta}/\epsilon} \\ &+ \sum_{n=1}^{\infty}\frac{2n\tilde{\beta}\epsilon^n\left(\varphi_n\cos n\theta + \hat{\varphi}_n\sin n\theta\right)}{\left(\epsilon\tilde{\alpha} + n\tilde{\beta}\right) - (\epsilon/R)^{2n}\left(\epsilon\tilde{\alpha} - n\tilde{\beta}\right)} \ . \end{aligned} \tag{56}$$

Now, it is enough to calculate the normal and tangential derivatives of u_ϵ on ∂B_ϵ, that is

$$\begin{aligned} \left.\frac{\partial u_\epsilon}{\partial n}\right|_{\partial B_\epsilon} = \left.\frac{\partial v_\epsilon}{\partial n}\right|_{\partial B_\epsilon} &= -\left.\frac{\partial v_\epsilon}{\partial r}\right|_{r=\epsilon} \\ &= \frac{\tilde{b}}{2}\epsilon - \frac{1}{\epsilon}\left(\frac{\tilde{\alpha}\frac{\tilde{b}}{4}(R^2-\epsilon^2) + \tilde{\alpha}\varphi_0 - \tilde{h} + \tilde{\beta}\frac{\tilde{b}}{2}\epsilon}{\tilde{\alpha}(\ln R - \ln\epsilon) + \tilde{\beta}/\epsilon}\right) \\ &\quad - \sum_{n=1}^{\infty}\frac{2n\tilde{\alpha}\epsilon^n\left(\varphi_n\cos n\theta + \hat{\varphi}_n\sin n\theta\right)}{\left(\epsilon\tilde{\alpha} + n\tilde{\beta}\right) - (\epsilon/R)^{2n}\left(\epsilon\tilde{\alpha} - n\tilde{\beta}\right)} \ , \end{aligned} \tag{57}$$

$$\left.\frac{\partial u_\epsilon}{\partial t}\right|_{\partial B_\epsilon} = \left.\frac{\partial v_\epsilon}{\partial t}\right|_{\partial B_\epsilon} = \left.\frac{1}{r}\frac{\partial v_\epsilon}{\partial\theta}\right|_{r=\epsilon} = \sum_{n=1}^{\infty}\frac{2n^2\tilde{\beta}\epsilon^{n-1}\left(\hat{\varphi}_n\cos n\theta - \varphi_n\sin n\theta\right)}{\left(\epsilon\tilde{\alpha} + n\tilde{\beta}\right) - (\epsilon/R)^{2n}\left(\epsilon\tilde{\alpha} - n\tilde{\beta}\right)} \ . \tag{58}$$

With these results in hand (Eqs. 56, 57, 58), the limit with $\epsilon \to 0$ in Eq. (54) can be calculated, in order to obtain the final expression of the Topological Derivative. It is important to mention that the solution defined in the domain Ω (without hole) will be denoted by u.

5.3.1 Neumann boundary condition on the hole ($\beta = 1, \alpha = \gamma = 0$)

Making $\beta = 1, \alpha = \gamma = 0$ and substituting in the Eq. (54) one has that

$$D_T(\hat{\mathbf{x}})_N = \frac{1}{2}\lim_{\epsilon\to 0}\frac{1}{f'(\epsilon)}\int_{\partial B_\epsilon}\left[k\left(\frac{\partial u_\epsilon}{\partial n}\right)^2 - k\left(\frac{\partial u_\epsilon}{\partial t}\right)^2 + 2bu_\epsilon + \frac{2}{\epsilon}\bar{q}^\epsilon u_\epsilon\right]d\partial B_\epsilon \ . \tag{59}$$

Taking into account that, in this case, $-k\partial u_\epsilon/\partial n = \bar{q}^\epsilon$ on ∂B_ϵ, the Eq. (59) remains

$$D_T(\hat{\mathbf{x}})_N = \frac{1}{2}\lim_{\epsilon\to 0}\frac{1}{f'(\epsilon)}\int_{\partial B_\epsilon}\left[\frac{\bar{q}^{\epsilon\,2}}{k} - k\left(\frac{\partial u_\epsilon}{\partial t}\right)^2 + 2bu_\epsilon + \frac{2}{\epsilon}\bar{q}^\epsilon u_\epsilon\right] d\partial B_\epsilon \ . \tag{60}$$

Considering $\bar{q}^\epsilon = 0$ (Neumann homogeneous boundary condition) and substituting the Eqs. (56,58) in the Eq. (60) one observes that the solution u_ϵ is non-singular. Hence,

$$f'(\epsilon) = -2\pi\epsilon \Rightarrow f(\epsilon) = -\pi\epsilon^2$$

and applying the localization theorem (see, for instance, Gurtin [11]), one obtains

$$D_T(\hat{\mathbf{x}})_{N_0} = k\nabla u(\hat{\mathbf{x}})\cdot\nabla u(\hat{\mathbf{x}}) - bu(\hat{\mathbf{x}}) \ . \tag{61}$$

In the same way, for $\bar{q}^\epsilon \neq 0$ (Neumann non-homogeneous boundary condition), one has

$$f'(\epsilon) = -2\pi \Rightarrow f(\epsilon) = -2\pi\epsilon$$

and then

$$D_T(\hat{\mathbf{x}})_N = -\bar{q}^\epsilon u(\hat{\mathbf{x}}) \ . \tag{62}$$

where u is the solution defined in the original domain Ω.

5.3.2 Robin boundary condition on the hole ($\gamma = 1, \alpha = \beta = 0$)

For $\gamma = 1, \alpha = \beta = 0$ the Eq. (54) provides

$$D_T(\hat{\mathbf{x}})_R = \frac{1}{2}\lim_{\epsilon\to 0}\frac{1}{f'(\epsilon)}\int_{\partial B_\epsilon}\left[k\left(\frac{\partial u_\epsilon}{\partial n}\right)^2 - k\left(\frac{\partial u_\epsilon}{\partial t}\right)^2 + 2bu_\epsilon + \frac{1}{\epsilon}h_c^\epsilon u_\epsilon(u_\epsilon - 2u_\infty^\epsilon)\right] d\partial B_\epsilon \ . \tag{63}$$

Substituting the Eqs. (56,57,58) in the Eq. (63) one has that the dominant term is given, since u_ϵ is non-singular, by

$$\frac{1}{\epsilon}h_c^\epsilon u_\epsilon(u_\epsilon - 2u_\infty^\epsilon) \ ,$$

then,

$$f'(\epsilon) = -2\pi \Rightarrow f(\epsilon) = -2\pi\epsilon$$

and, applying the localization theorem, one obtains

$$D_T(\hat{\mathbf{x}})_R = -\frac{1}{2}h_c^\epsilon u(\hat{\mathbf{x}})(u(\hat{\mathbf{x}}) - 2u_\infty^\epsilon) \ . \tag{64}$$

5.3.3 Dirichlet boundary condition on the hole ($\alpha = 1, \beta = \gamma = 0$)

Making $\alpha = 1, \beta = \gamma = 0$ and substituting in the Eq. (54) one has that

$$D_T(\hat{\mathbf{x}})_D = \frac{1}{2}\lim_{\epsilon\to 0}\frac{1}{f'(\epsilon)}\int_{\partial B_\epsilon}\left[k\left(\frac{\partial u_\epsilon}{\partial n}\right)^2 - k\left(\frac{\partial u_\epsilon}{\partial t}\right)^2 + 2bu_\epsilon\right] d\partial B_\epsilon \ . \tag{65}$$

Taking into account that on ∂B_ϵ, $u_\epsilon = \bar{u}^\epsilon$ and that $\partial u_\epsilon/\partial t = 0$ (see Eq. 58), the Eq. (65) remains

$$D_T(\hat{\mathbf{x}})_D = \frac{1}{2}\lim_{\epsilon\to 0}\frac{1}{f'(\epsilon)}\int_{\partial B_\epsilon}\left[k\left(\frac{\partial u_\epsilon}{\partial n}\right)^2 + 2b\bar{u}^\epsilon\right] d\partial B_\epsilon \ . \tag{66}$$

In this case, from the Eq. (57) one observes that the solution u_ϵ is singular[3], that is, the dominant term is given by $k(\partial u_\epsilon/\partial n)^2$ and $\partial u_\epsilon/\partial n$ is such that

$$\lim_{\epsilon \to 0} \left[\frac{\partial u_\epsilon}{\partial n} \epsilon \ln(\epsilon) \right] = u(\hat{\mathbf{x}}) - \bar{u}^\epsilon \ .$$

Therefore, one observes that

$$f'(\epsilon) = -\frac{2\pi}{\epsilon \ln(\epsilon)^2} \Rightarrow f(\epsilon) = \frac{2\pi}{\ln(\epsilon)} \ .$$

Considering this last result and substituting the Eq. (57) in the Eq. (66), one has, after applying the localization theorem, that

$$D_T(\hat{\mathbf{x}})_D = -\frac{1}{2} k \left(u(\hat{\mathbf{x}}) - \bar{u}^\epsilon \right)^2 \ . \tag{67}$$

5.4 Summary of the results

A summary of the obtained results is shown in the Table 1, where one has the final expressions of the Topological Derivatives for the Poisson's problem, which were obtained via Shape Sensitivity Analysis (Theorem 1), considering the various types of boundary conditions studied (Eqs. 61, 62, 64, 67), taking as a cost function the total potential energy (Eq. 41).

Table 1: Topological Derivatives in $2D$ Poisson's problem, for Neumann ($\beta = 1, \alpha = \gamma = 0$), Robin ($\gamma = 1, \alpha = \beta = 0$) or Dirichlet ($\alpha = 1, \beta = \gamma = 0$) boundary condition on the hole and considering the total potential energy as the cost function.

Boundary Conditions	$f(\epsilon)$	D_T
$\beta = 1, \alpha = \gamma = 0$ and $\bar{q}^\epsilon = 0$	$-\pi\epsilon^2$	$k\nabla u \cdot \nabla u - bu$
$\beta = 1, \alpha = \gamma = 0$ and $\bar{q}^\epsilon \neq 0$	$-2\pi\epsilon$	$-\bar{q}^\epsilon u$
$\gamma = 1, \alpha = \beta = 0$	$-2\pi\epsilon$	$-\frac{1}{2} h_c^\epsilon u (u - 2u_\infty^\epsilon)$
$\alpha = 1, \beta = \gamma = 0$	$\frac{2\pi}{\log(\epsilon)}$	$-\frac{1}{2} k (u - \bar{u}^\epsilon)^2$

From the analysis of the Table 1 one observes that it is sufficient to calculate the solution of the original problem (without hole), that is u, to obtain the sensitivity of the cost function when a hole is created in an arbitrary point $\hat{\mathbf{x}} \in \Omega$. Thus, the Topological Derivative can be obtained without additional cost, besides that necessary in the calculation of u and λ and/or ∇u and $\nabla \lambda$ (note that in

[3]In the Saint-Venant theory of torsion of elastic shaft, which may also be modeled through the Poisson's equation, one has a very special case of Dirichlet boundary condition that doesn't originate singularities in the solution.

this case $\lambda = 0$ due to the choice of a particular cost function, as can be seen in Eq. 42). Another important consequence of the Theorem 1 is that the Topological Derivative can be calculated in more complex cases than the one here considered: in cases where it is not possible to make an Asymptotic Analysis of the solution. In fact, the Shape Sensitivity Analysis can be realized without further problems in such situations and the limit with $\epsilon \to 0$, that appears in the Eq. (16), can be calculated employing an appropriate numerical method.

6 Numerical experiments

In this work, it was firstly shown the relation between the Topological Derivative and the Shape Sensitivity Analysis, leading to the Topological-Shape Sensitivity Analysis (Section 4). Soon after, in Section 5, the calculation of the Topological Derivative was performed for the Poisson's problem (Eq. 27), considering as a constraint the state equation in its weak form (Eq. 30) and as a cost function the total potential energy (Eq. 41). This objective function can be interpreted, in this case, as a measure of the heat flux, or even, as a measure of energy in transit in the body under analysis.

Then, the goal of this Section is to point out, by several numerical experiments, the effectiveness of the information given by the Topological Derivatives summarized in Table 1. In fact, this derivative gives the information on the opportunity to create a small hole in the domain. Therefore, as stated in the works of Céa et al. [4] and Garreau et al. [10], the function $D_T(\hat{\mathbf{x}})$ can be used similarly to a descent direction in a topology optimization process (for a survey on topology optimization methods, the reader is referred to the review paper by Eschenauer et. al. [5]). However, it is easy to see that, in the manner as shown in the present work, it is still necessary to consider some additional constraint in the problem, besides the state equation, in order to avoid that any iterative procedure leads merely to the trivial solution of the problem, *i.e.* $meas\,(\Omega) = 0$. A simple way to outline this problem consists in introducing a *Stop Criterion* in the process. Thus, following [4, 10], the iterative procedure to be used in the numerical experiments can be stated as:

Considering the sequence $\{\Omega^j\}$, where j is the j-th iteration, then:

1. Provide the initial domain Ω and the *Stop Criterion*.
2. While the *Stop Criterion* is not satisfied do:
   - **(a)** Find the solution u^j associated to the domain Ω^j.
   - **(b)** Calculate $D_T\left(\hat{\mathbf{x}}\right)^j$ according to Table (1).
   - **(c)** Create the holes in the points $\hat{\mathbf{x}}$ corresponding to $\eta^j_{\text{inf}} \leq D_T\left(\hat{\mathbf{x}}\right)^j \leq \eta^j_{\text{sup}}$, where η^j_{inf} and η^j_{sup} are specify proportionally to the volume of material to be removed in each iteration j.
   - **(d)** Define the new domain Ω^{j+1}.
   - **(e)** Make $j \leftarrow j + 1$.
3. At this stage, it is hoped to have in hand the desired final design.

As can be seen in Table 1, the Topological Derivative $D_T\left(\hat{\mathbf{x}}\right)$ depends on the $u\left(\hat{\mathbf{x}}\right)$ and/or $\nabla u\left(\hat{\mathbf{x}}\right)$, the source b and the boundary conditions on ∂B_ϵ. In this work, the solution $u\left(\hat{\mathbf{x}}\right)$ is calculated via Finite Element Method (see, for instance, Szabó & I. Babuška [20]), that is, $u\left(\hat{\mathbf{x}}\right) \approx u_h\left(\hat{\mathbf{x}}\right)$ and $\nabla u\left(\hat{\mathbf{x}}\right) \approx \nabla u_h\left(\hat{\mathbf{x}}\right)$, where $\nabla u_h\left(\hat{\mathbf{x}}\right)$ is obtained by a post-processing of the approximated solution $u_h\left(\hat{\mathbf{x}}\right)$, such as proposed in the work of Hinton & Campbell [12]. More specifically, in the following examples the three node triangular finite element is adopted for the discretization of the estate equation (see, for instance, Zienkiewicz & Taylor [22] and Hughes [13]). Furthermore, the Topological Derivative $D_T\left(\hat{\mathbf{x}}\right)$ is evaluated on the nodal points of the finite elements mesh, being that the elements that share the

node which satisfies $\eta_{\text{inf}} \leq D_T(\hat{\mathbf{x}}) \leq \eta_{\text{sup}}$ are eliminated, in the way of creating the holes in the finite elements mesh (for more technical details, see the work of Novotny [15]). This procedure, already proposed by Céa et al. [4] and Garreau et al. [10], is essentially the so-called *hard-kill* method, also discussed in [5].

6.1 Example 1 - design of heat conductors

In this example, three distinct cases will be analyzed, where, in all of them, a domain $\Omega = (0, 10) \times (0, 10)$ will be considered, whose contour is given by $\partial\Omega = \Gamma_D \cup \Gamma_N$, where $\Gamma_D = \Gamma_{D_1} \cup \Gamma_{D_2}$ and $meas(\Gamma_{D_1}) = meas(\Gamma_{D_2}) = 4$. On Γ_N one has that $\bar{q} = 0$ and on Γ_{D_1} and Γ_{D_2} are prescribed the temperatures $\bar{u}_1 = 0$ and $\bar{u}_2 = 100$, respectively. In the holes created via Topological Derivative, Neumann homogeneous boundary conditions are imposed, that is, $\bar{q}^\epsilon = 0$ on ∂B_ϵ, hence, the Topological Derivative will be calculated by the Eq. (61), considering $b = 0$ and $k = 1$, *i.e.*:

$$D_T(\hat{\mathbf{x}})_{N_0} \approx \nabla u_h(\hat{\mathbf{x}}) \cdot \nabla u_h(\hat{\mathbf{x}}) \ .$$

Therefore, the idea is to create holes where the cost function given by Eq. (41) is **less** sensible, that is, where $D_T(\hat{\mathbf{x}})$ assumes the **smallest** values. In this way, it is desired to obtain different configurations of heat conductors, depending as how Γ_{D_1} and Γ_{D_2} are disposed on $\partial\Omega$. The adopted *Stop Criterion* is over the final volume to be obtained. That is, the idea is creating the holes while $meas(\Omega) \geq meas(\hat{\Omega})$, where $meas(\hat{\Omega})$ corresponds to the final volume required. In all cases to be analyzed, 0.5% of material shall be removed at each iteration.

- **Case A**: The initial domain Ω and the disposition of Γ_{D_1} and Γ_{D_2} are presented in Fig. (4a). The finite elements mesh used to discretize Ω can be seen in Fig. (4b).

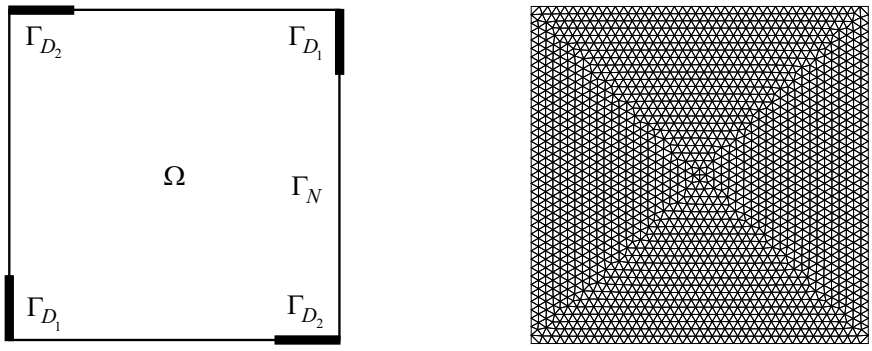

(a) initial domain Ω (b) mesh

Figure 4: Example 1 - Case A: model and mesh with 3656 finite elements.

In this case, the adopted stop criterion is given by $meas(\hat{\Omega}) = 0.8\, meas(\Omega)$. The Topological Derivatives calculated in the iterations $j = 0$, $j = 10$, $j = 20$ and $j = 35$ are shown in Fig. (5), where one observes a heat conductor that divides the flux, directing it from Γ_{D_2} to Γ_{D_1}, as can be seen in Fig. (6).

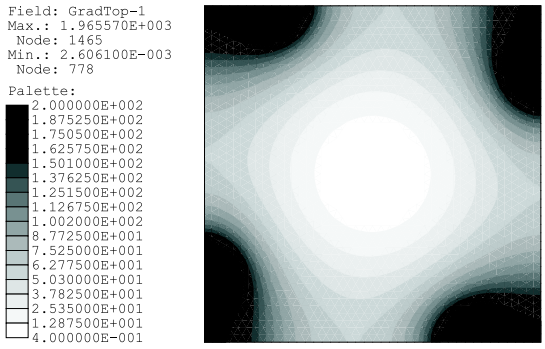

(a) Topological Derivative at $j = 0$

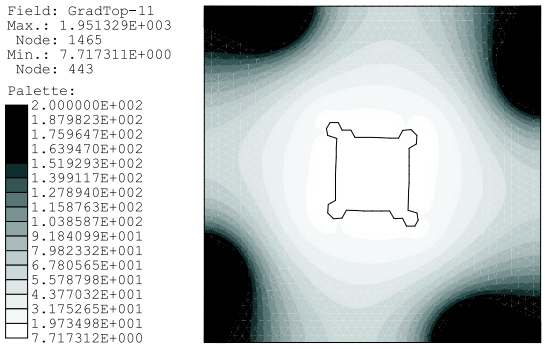

(b) Topological Derivative at $j = 10$

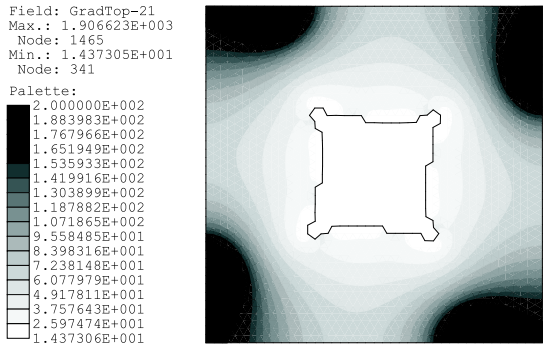

(c) Topological Derivative at $j = 20$

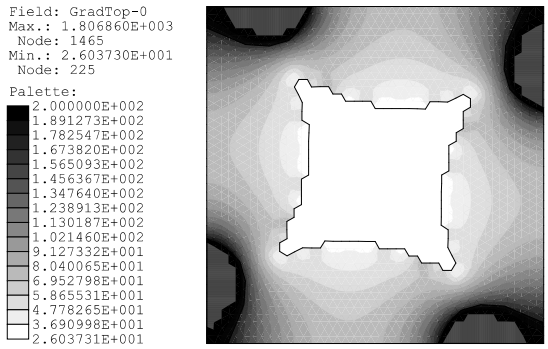

(d) Topological Derivative at $j = 35$

Figure 5: Example 1 - Case A: obtained result.

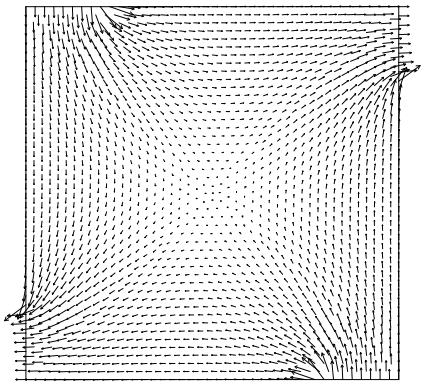

(a) heat flux at $j = 0$

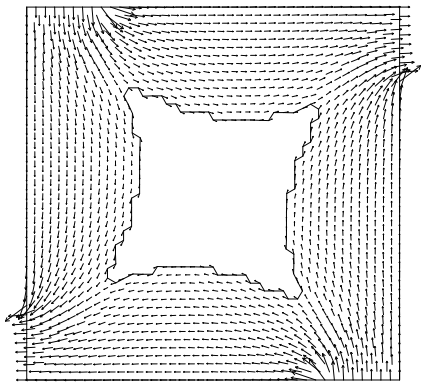

(b) heat flux at $j = 35$

Figure 6: Example 1 - Case A: heat flux.

In Fig. (7) is shown the cost function (total potential energy) calculated in each iteration, where one note that it diminishes during the iterative process.

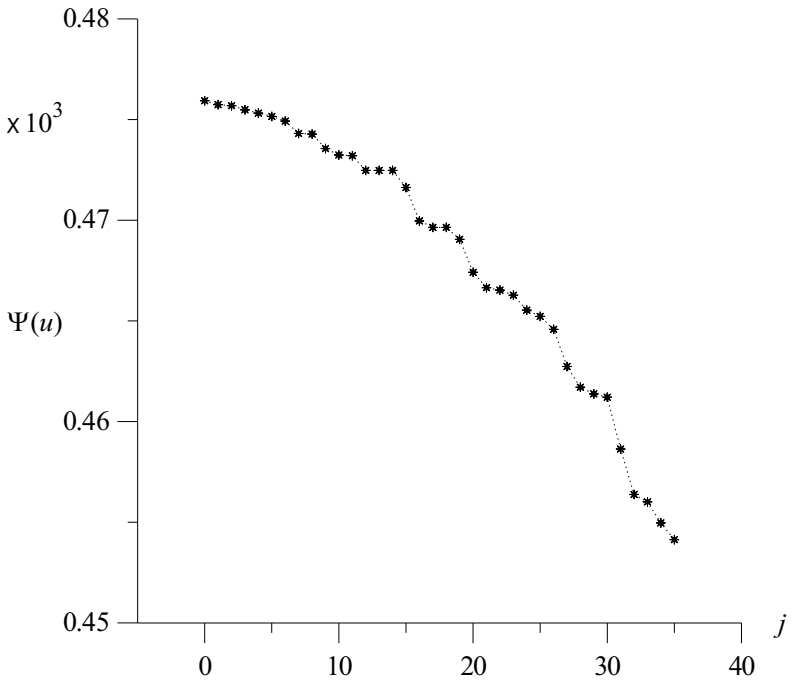

Figure 7: Example 1 - Case A: cost function $\Psi(u)$ in each iteration.

- **Case B**: The Fig. (8a) shows the disposition of Γ_{D_1} and Γ_{D_2} and the initial domain Ω, having a hole B_R in it baricenter, whose radius is $R = 2$. Due to the symmetry of the problem, only half of Ω is discretize, as can be seen in Fig. (8b).

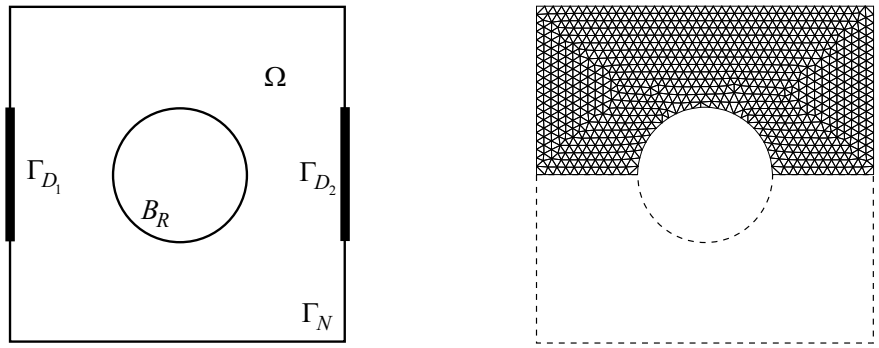

(a) initial domain Ω (b) mesh

Figure 8: Example 1 - Case B: model and mesh with 1583 finite elements.

The Topological Derivative calculated in the first iteration ($j = 0$) can be seen in Fig. (9a). In Fig. (9b) is shown the design obtained in the last iteration ($j = 56$), considering $meas(\hat{\Omega}) = 0.7\, meas(\Omega)$. As in the previous case, one also observes a heat conductor that directs the flux from Γ_{D_2} to Γ_{D_1} (see Fig. 10)

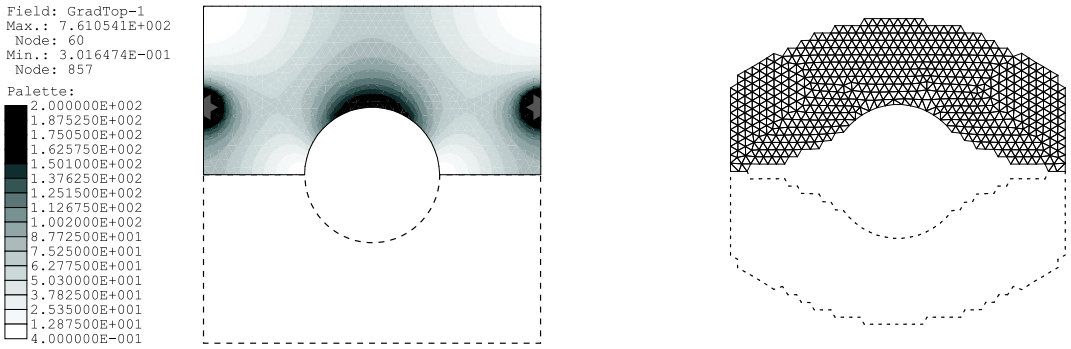

(a) Topological Derivative at $j = 0$ (b) final domain Ω^{56}

Figure 9: Example 1 - Case B: obtained result.

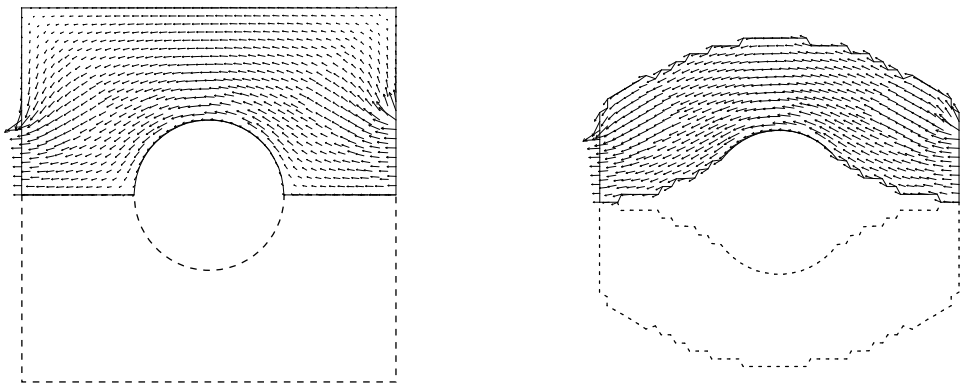

(a) heat flux at $j = 0$ (b) heat flux at $j = 56$

Figure 10: Example 1 - Case B: heat flux.

- **Case C**: In Fig. (11a) is presented the initial domain Ω, as well as the disposition of Γ_{D_1} and Γ_{D_2}. Due to the symmetry of the problem, only half of Ω is discretized, as can be seen in Fig. (11b).

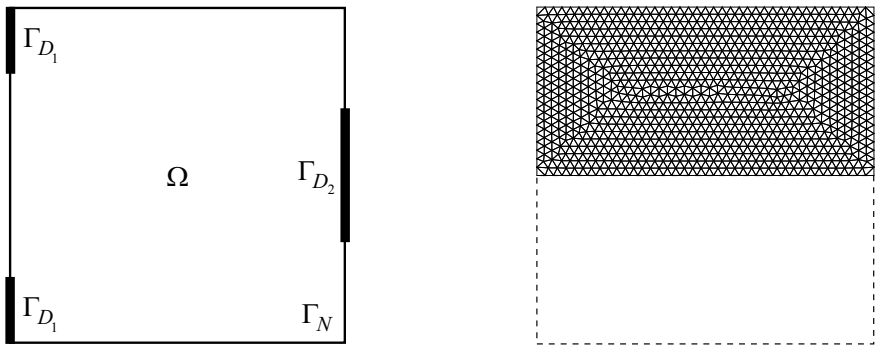

(a) initial domain Ω (b) mesh

Figure 11: Example 1 - Case C: model and mesh with 1822 finite elements.

The Topological Derivative calculated in the first iteration is shown in Fig. (12a). The design obtained in the last iteration ($j = 78$), considering $meas(\hat{\Omega}) = 0.6\, meas(\Omega)$, is presented in Fig. (12b), where one clearly observes, again, a heat conductor that directs the flux from Γ_{D_2} to Γ_{D_1}.

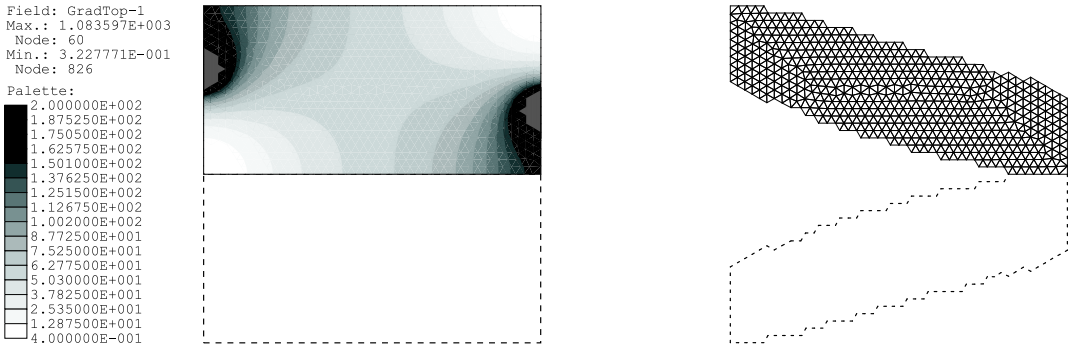

(a) Topological Derivative at $j = 0$

(b) final domain Ω^{78}

Figure 12: Example 1 - Case C: obtained result.

This example, although academic, shows that the Topological Derivative can be used to determine where the holes must be positioned, in order to automatically design components able to *channel* the heat flux from Γ_{D_2} (hotter region) to Γ_{D_1} (more cold region).

6.2 Example 2 - design of a heat exchanger

In this example, one seeks to design a heat exchanger. Accordingly, it is necessary to create the holes where the cost function (Eq. 41) is **more** sensible, that is, where $D_T(\hat{\mathbf{x}})$ assumes the **greatest** absolute values. In practice, the Neumann or Dirichlet boundary conditions on ∂B_ϵ are very severe hypothesis, the reason for which only the Robin boundary conditions shall be imposed on ∂B_ϵ, whose Topological Derivative is given by Eq. (64), that is,

$$D_T(\hat{\mathbf{x}})_R \approx -\frac{1}{2} h_c^\epsilon u_h(\hat{\mathbf{x}}) \left(u_h(\hat{\mathbf{x}}) - 2u_\infty^\epsilon\right) ,$$

The problem being considered can be seen in Fig. (13), where one has a body denoted by Ω, whose thermal conductivity is such that $k = 204W/(m\,^oC)$, and a cooling surface, Γ_R, which is exposed to the ambient air (steady air) at a temperature $u_\infty = 25^oC$, leading to a heat-transfer coefficient $h_c = 20W/\left(m^2\,^oC\right)$. When a cooling channel is introduced, one has water at a temperature $u_\infty^\epsilon = 30^oC$, that flows throughout the interior of it, in order to induce a heat-transfer coefficient $h_c^\epsilon = 200W/\left(m^2\,^oC\right)$. Finally, the heat flux $\bar{q}$ prescribed on Γ_N presents a piecewise linear distribution, where the smallest value is $\bar{q}_1 = 2 \times 10^3 W/m^2$ and the greatest value is $\bar{q}_2 = 2 \times 10^4 W/m^2$. Due to the periodical symmetry of the problem, only a part $2L \times L$, where $L = 4m$, of the whole domain is discretized (see mesh shown in Fig. 13), and the gray region of width $a = 1m$ each one, shown in the same figure, shall not be perturbed, being considered the structural part of the problem.

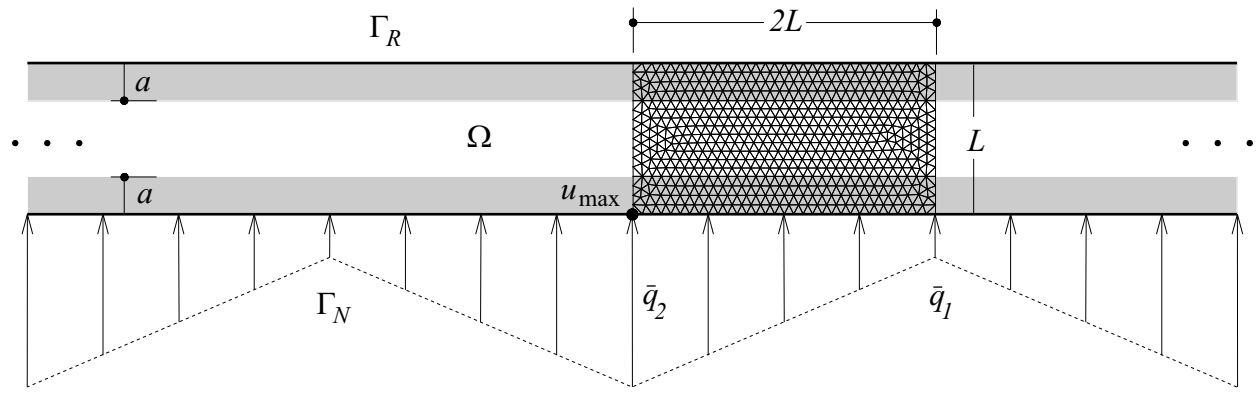

Figure 13: Example 2: model and mesh with 1086 finite elements.

If the holes are created where the cost function (Eq. 41) is more sensible, then the maximum temperature, denoted by $u_{\max}$ in Fig. (13), should be diminished up to the required value $u^*_{\max}$. Then, the idea is to change the design of the structure, by introducing holes, up to $u_{\max} \leq u^*_{\max}$. Considering this condition as the *Stop Criterion* to be adopted, where $u^*_{\max} = 200^oC$, and removing 1% of the material in each iteration, one observes that the temperature $u_{\max}$ actually diminishes during the iterative process, which can be seen in Fig. (14).

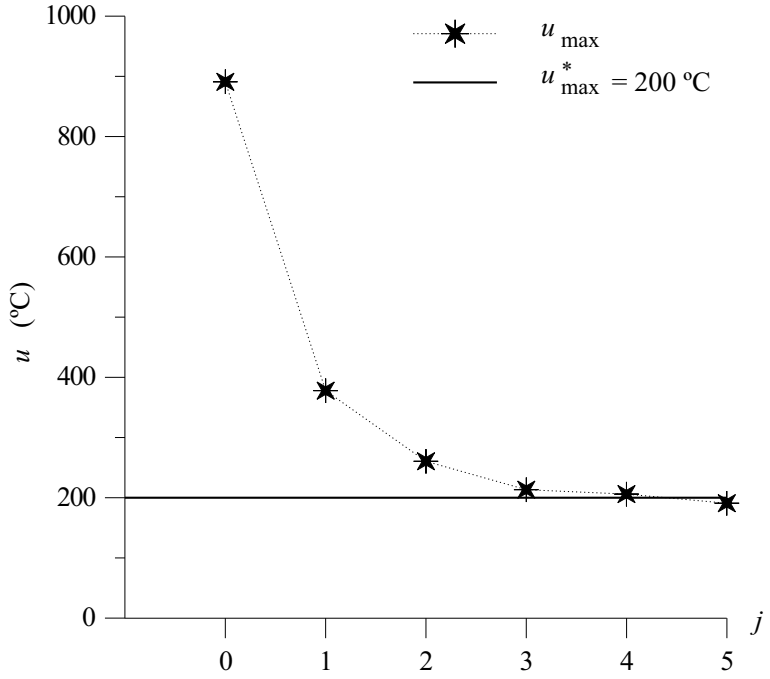

Figure 14: Example 2: maximum temperature (u_{max}) in each iteration.

Through analysis of Fig. (14), one notes that the condition $u_{\max} < u^*_{\max}$ is reached in the iteration $j = 5$, from which $u_{\max}$ presents an asymptotic behavior. Thus, if the required temperature were $u^*_{\max} << 200^oC$ ($u^*_{\max} = 100^oC$, for instance), the flow condition imposed into the cooling channels (represented by the parameters h^ϵ_c and u^ϵ_∞) would be insufficient to reach it.

The temperature distribution obtained in each iteration is shown in Fig. (15), where one observes a diminution of the temperature in the whole domain, as the cooling channels are being automatically introduced via Topological Derivative, whose distribution calculated in each iteration can be seen in Fig. (16).

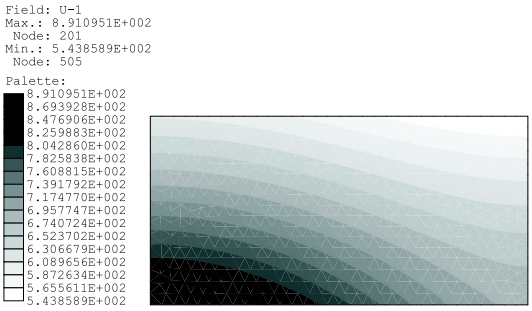

(a) temperature at $j = 0$

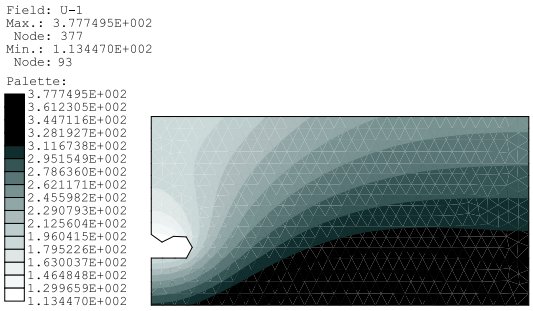

(b) temperature at $j = 1$

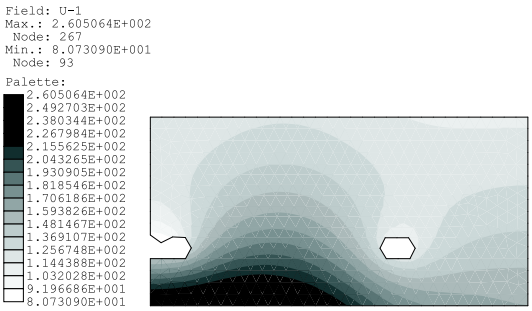

(c) temperature at $j = 2$

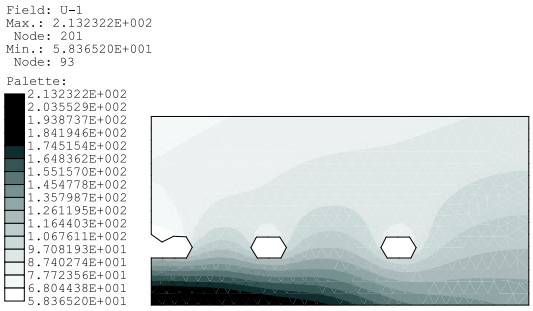

(d) temperature at $j = 3$

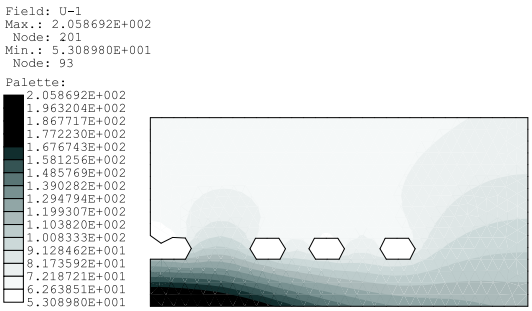

(e) temperature at $j = 4$

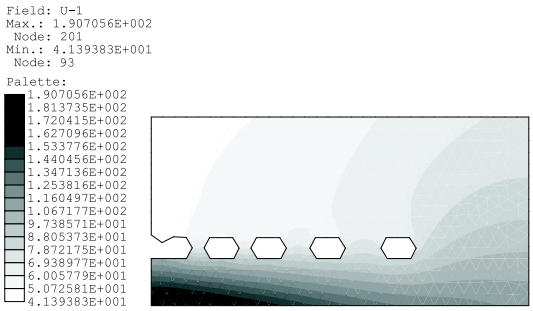

(f) temperature at $j = 5$

Figure 15: Example 2: temperature distribution obtained during the iterative process.

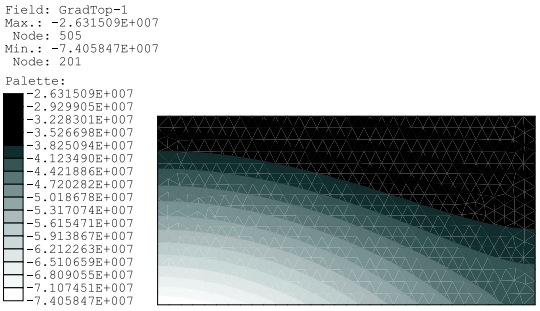

(a) Topological Derivative at $j = 0$

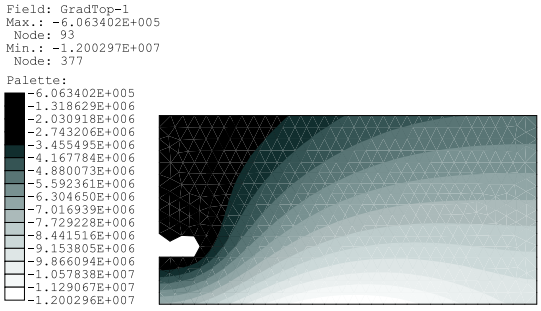

(b) Topological Derivative at $j = 1$

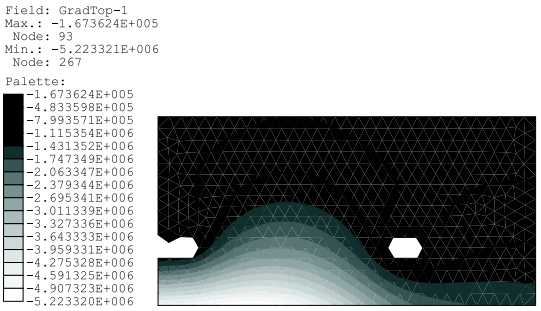

(c) Topological Derivative at $j = 2$

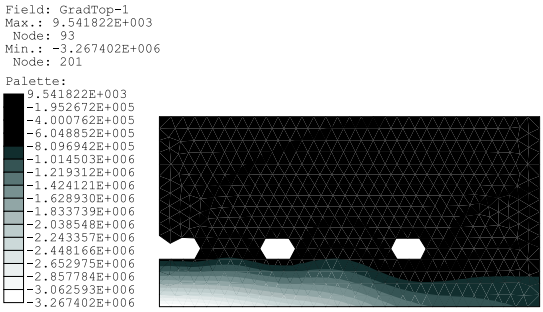

(d) Topological Derivative at $j = 3$

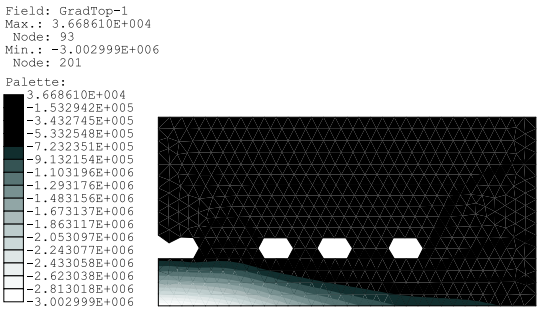

(e) Topological Derivative at $j = 4$

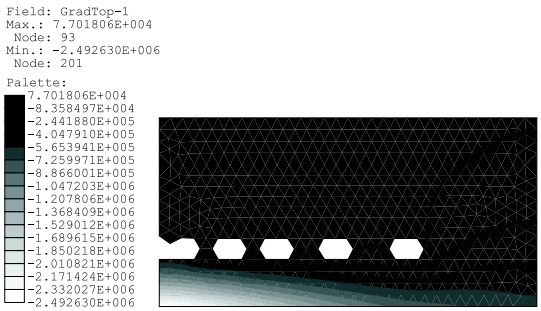

(f) Topological Derivative at $j = 5$

Figure 16: Example 2: Topological Derivative obtained during the iterative process.

The final design obtained in the iteration $j = 5$ is presented in Fig. (17), where one notes that the distance between the channels grows as these stand back from the point of maximum temperature, as it was expected.

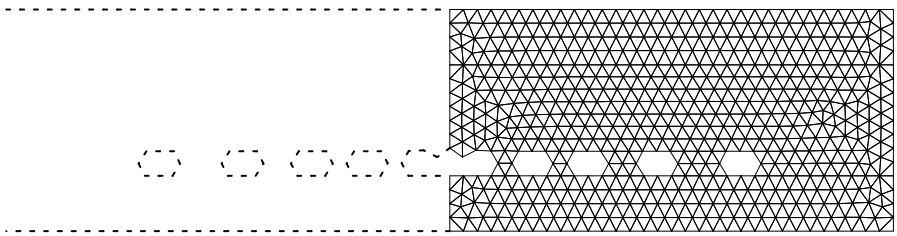

Figure 17: Example 2 - final design.

This example shows how the Topological Derivative can be utilized to design heat exchangers, in order to automatically determinate where the cooling channels must be positioned, satisfying some requirement.

Now, considering that the fluid flows throughout the channels in such high velocity that induces a heat-transfer coefficient $h_c^\epsilon \to \infty$, the Newton's law of cooling degenerates to a Dirichlet boundary condition on the holes, that is $\bar{u}^\epsilon = u_\infty^\epsilon$, where $\bar{u}^\epsilon$ is the prescribed temperature on ∂B_ϵ. Thus, this same problem will be analyzed considering the Dirichlet boundary condition on ∂B_ϵ, whose Topological Derivative if given by Eq. (67), that is

$$D_T\left(\hat{\mathbf{x}}\right)_D \approx -\frac{1}{2}k\left(u_h\left(\hat{\mathbf{x}}\right) - \bar{u}^\epsilon\right)^2 \ ,$$

where $\bar{u}^\epsilon = 30^oC$.

The Topological Derivative calculated in the iteration $j = 0$ and $j = 5$ are shown in Fig. (18).

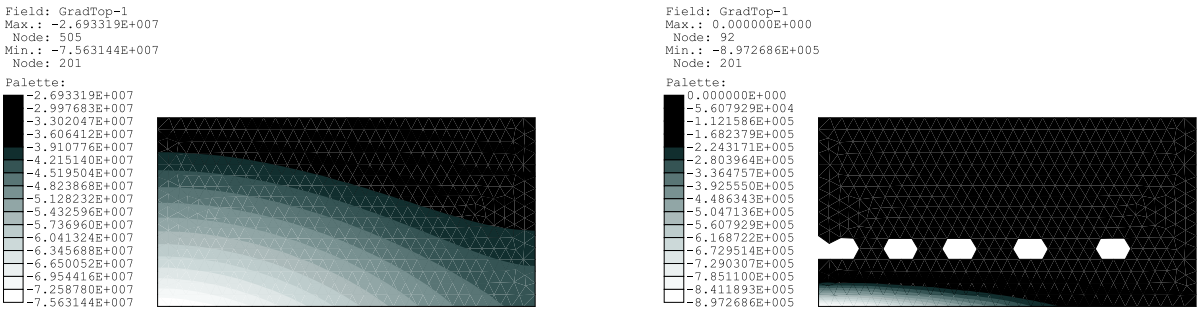

(a) Topological Derivative at $j = 0$ (b) Topological Derivative at $j = 5$

Figure 18: Example 2: Topological Derivative obtained in the first (a) and in the last (b) iterations, considering the Dirichlet boundary condition on the holes.

The temperature distribution obtained in the last iteration ($j = 5$) is presented in Fig. (19a), where one has that $u_{\max} \approx 124^oC << u_{\max}^*$, which was expected, since the Dirichlet boundary condition on the channels represents $h_c^\epsilon \to \infty$. The final design is shown in Fig. (19b), where it is possible to observe a distribution of the channels similar that the one already obtained.

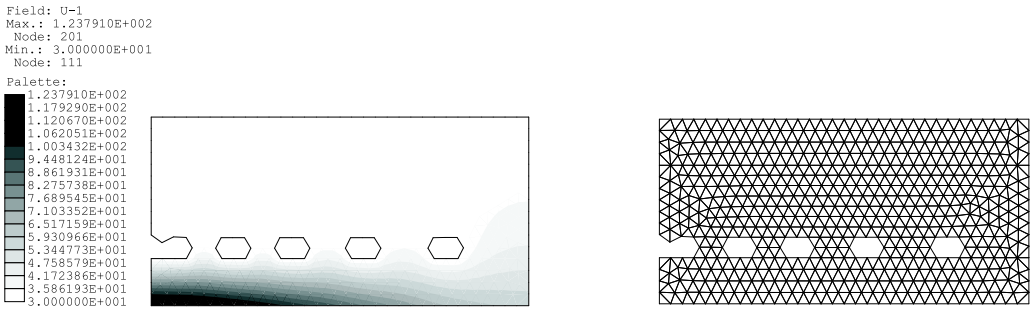

(a) temperatura at $j = 5$ (b) final design

Figure 19: Example 2: Temperature distribution calculated in the iteration $j = 5$ (a) and final design obtained (b), considering the Dirichlet boundary condition on the holes.

This last analysis shows that, even utilizing a very simplified model (Dirichlet boundary condition on the holes), one obtains satisfactory results, at least from the qualitative point of view.

7 Conclusions

In this work, Shape Sensitivity Analysis was employed to evaluate the Topological Derivative in an alternative way. The relationship between both concepts was formally demonstrated in Theorem

1, leading to the Topological-Shape Sensitivity Analysis. This theorem shows that the Topological Derivative is a generalization of the Shape Sensitivity Analysis concept. Therefore, as shown in Section 5, results obtained in Shape Sensitivity Analysis can be used to perform the Topological Derivative in a simple and constructive way.

In order to illustrate the potentialities of the result obtained in Theorem 1, the Topological Derivative was calculated, utilizing Eq. (16), for a steady-state heat conduction problem with total potential energy as the cost function. This is an adequate example since not only it has several practical applications, but one can also study the effects on the theory of different boundary conditions on the hole (Dirichlet, Neumann or Robin boundary conditions). It is important to mention that the extension of the methodology here proposed to other engineering problems (non-linear solid mechanics, fluid mechanics, electromagnetism, and so on) with general cost functions is straightforward.

The Topological-Shape Sensitivity Analysis, *i.e.* the Topological Derivative based on Shape Sensitivity Analysis, was expressed in terms of the limit $\epsilon \to 0$ in Eq. (54). To calculate this limit, it was necessary to make an asymptotic analysis of the solution u_ϵ and of its normal and tangential derivatives, which allowed to apply the localization theorem in Eq. (54) to obtain the results shown in Table 1. However, when it is not possible to perform an asymptotic analysis of the solution (for instance, in non-linear problems in general) the limit $\epsilon \to 0$ in Eq. (54) can be estimated numerically, allowing to extend the methodology proposed in this work to more complex problems.

Finally, in Section 6, the Topological Derivative was used to improve the design of heat conducting components, showing that it provides an useful information for positioning holes. This fact highlights that the Topological Derivative concept is a tool that can be applied in topology optimization algorithms, as pointed out by Eschenauer & Olhoff [5]. In addition, other strategies using the information provided by the Topological-Shape Sensitivity Analysis must be investigated. Among those, an strategy that exploits the eigenvectors of the tensor $\mathbf{\Sigma}$ will be studied in future works.

Acknowledgments

This research was partly supported by FINEP/CNPq-PRONEX (Brazil) Project under Contract 664007/1997-0 and by CONICET (Argentina). Antonio André Novotny was partially supported by Brazilian government fellowship from CNPq under Grant 141560/2000-2. The support from these agencies is greatly appreciated.

References

[1] M.P. Bendsøe & N. Kikuchi, Generating Optimal Topologies in Structural Design Using an Homogenization Method, Comput. Methods Appl. Mech. Engrg. 71 (1988), 197-224.

[2] M.P. Bendsøe, Optimal Shape Design as a Material Distribution Problem. Struct. Optim., 1 (1989), 193-202.

[3] D.E. Carlson, Linear Thermoelasticity (Springer-Verlag, 1972).

[4] J. Céa, S. Garreau, Ph. Guillaume & M. Masmoudi, Shape and Topological Optimizations Connection, Research Report, UFR MIG, Université Paul Sabatier, Toulouse, France, 1998. Also published in Comput. Methods Appl. Mech. Engrg. 188 (2000), 713-726.

[5] H.A. Eschenauer & N. Olhoff, Topology Optmization of Continuum Structures: A Review, Appl. Mech. Rev. 54 (2001), 331-390.

[6] H.A. Eschenauer, V.V. Kobelev & A. Schumacher, Buble Method for Topology and Shape Optmization of Structures, Structural Optimization, 8 (1994), 42-51.

[7] J.D. Eshelby, The Elastic Energy-Momentum Tensor, Journal of Elasticity 5 (1975), 321-335.

[8] E.A. Fancello, Análise de Sensibilidade, Geração Adaptativa de Malhas e o Método dos Elementos Finitos na Otimização de Forma em Problemas de Contato e Mecânica da Fratura, Doctoral Thesis, COPPE-UFRJ, Rio de Janeiro, Brasil, 1993.

[9] S. Garreau, Ph. Guillaume & M. Masmoudi, The Topological Gradient, Research Report, UFR MIG, Université Paul Sabatier, Toulouse, France, 1998.

[10] S. Garreau, Ph. Guillaume & M. Masmoudi, The Topological Asymptotic for PDE Systems: The Elasticity Case, SIAM J. Control Optim. 39 (2001), 1756-1778.

[11] M.E. Gurtin, An Introduction to Continuum Mechanics, Mathematics in Science and Engineering (Academic Press, New York, 1981).

[12] E. Hinton & J.S. Campbell, Local and Global Smoothing of Discontinuous Finite Element Functions Using a Least Square Method, Int. J. Num. Methods Engrg. 8 (1974), 461-480.

[13] T.J.R. Hughes, The Finite Element Method - Linear Static and Dynamic Finite Element Analysis (Prentice-Hall, New Jersey, 1987).

[14] F. Murat & J. Simon, Sur le Contrôle par un Domaine Géométrique, Doctoral Thesis, Université Pierre et Marie Curie, Paris, France, 1976.

[15] A.A. Novotny, Adaptividade h na Otimização Topológica e Projeto Ótimo de Malhas hp Adaptativas, Master Thesis, GRANTE-EMC-UFSC, Florianópolis, Brasil, 1998.

[16] A. Schumacher, Topologieoptimierung von Bauteilstrukturen unter Verwendung von Lochpositionierungkriterien, Doctoral Thesis, FOMMAS-Report Nr T09-01.96. Univ of Siegen, 1996.

[17] J.C. Slattery, Advanced Transport Phenomena (McGraw Hill, 1997).

[18] J. Sokolowski & A. Żochowski, On Topological Derivative in Shape Optimization, SIAM J. Control Optim. 37 (1999), 1251-1272.

[19] J. Sokolowski & A. Żochowski, Topological Derivatives for Elliptic Problems, Inverse Problems, 15 (1999), 123-134.

[20] B. Szabó & I. Babuška, Finite Element Analysis (John Wiley & Sons, New York, 1991).

[21] E. Taroco, G. Buscaglia and R.A. Feijóo, Second Order Shape Sensitivity Analysis for Non-Linear Problems, Int. J. for Structural Optimization, 15 (1998), 101-113.

[22] O.C. Zienkiewicz & R. L. Taylor, The Finite Element Method, vols. 1 and 2 (McGraw Hill, 1989).

[23] J.P. Zolézio, The Material Derivative (or Speed) Method for Shape Optimization. In Optimization of Distributed Parameters Structures. Iowa, 1981.